Pluripotent stem cell model of early hematopoiesis in Down syndrome reveals quantitative effects of short-form GATA1 protein on lineage specification

Shiori Matsuo [1], Yoko Nishinaka-Arai [1,5,*], Yasuhiro Kazuki [2,3], Mitsuo Oshimura [2], Tatsutoshi Nakahata[4], Akira Niwa [1,*] and Megumu K. Saito [1,*]

[1] Department of Clinical Application, Center for iPS cell Research and Application, Kyoto University, Kyoto, Japan

[2] Chromosome Engineering Research Center, Tottori University, Tottori, Japan

[3] Division of Genome and Cellular Functions, Department of Molecular and Cellular Biology, School of Life Science, Faculty of Medicine, Tottori University, Tottori, Japan

[4] Drug Discovery Technology Development Office, Center for iPS cell Research and Application, Kyoto University, Kyoto, Japan

[5] Department of Human Health Sciences, Graduate School of Medicine, Kyoto University, Kyoto, Japan

[*] Corresponding authors

Category for the Table of Contents *Nonmalignant Hematologic diseases, Hematologic Malignancies*

Keywords *Transient abnormal myeloid proliferation, Down syndrome-related megakaryoblastic leukemia, short-form GATA1*

Address for Correspondence

Megumu K. Saito, M.D., Ph.D., Akira Niwa, M.D., Ph.D. or Yoko Nishinaka-Arai

Center for iPS Cell Research and Application (CiRA), Kyoto University

53, Shogoin-Kawahara-cho, Sakyo-ku, Kyoto, Japan

Phone: +81-75-366-7085

FAX : +81 -75-366-7091

E-mail : msaito@cira.kyoto-u.ac.jp

akiranw@cira.kyoto-u.ac.jp

Abstract

Children with Down syndrome (DS) are susceptible to two blood disorders, transient abnormal myelopoiesis (TAM) and Down syndrome-associated acute megakaryocytic leukemia (DS-AMKL). Mutations in *GATA binding protein 1* (*GATA1*) have been identified as the cause of these diseases, and the expression levels of the resulting protein, short-form GATA1 (GATA1s), are known to correlate with the severity of TAM. On the other hand, despite the presence of *GATA1* mutations in almost all cases of DS-AMKL, the incidence of DS-AMKL in TAM patients is inversely correlated with the expression of GATA1s. This discovery has required the need to clarify the role of GATA1s in generating the cells of origin linked to the risk of both diseases. Focusing on this point, we examined the characteristics of *GATA1* mutant trisomy-21 pluripotent stem cells transfected with a doxycycline (Dox)-inducible GATA1s expression cassette in a stepwise hematopoietic differentiation protocol. We found that higher GATA1s expression significantly reduced commitment into the megakaryocytic lineage at the early hematopoietic progenitor cell (HPC) stage, but once committed, the effect was reversed in progenitor cells and acted to maintain the progenitors. These differentiation stage-dependent reversal effects were in contrast to the results of myeloid lineage, where GATA1s simply sustained and increased the number of immature myeloid cells. These results suggest that although *GATA1* mutant cells cause the increase in myeloid and megakaryocytic progenitors regardless of the

53 intensity of GATA1s expression, the pathways vary with the expression level. This study provides

54 experimental support for the paradoxical clinical features of *GATA1* mutations in the two diseases.

55

Introduction

Children with Down syndrome (DS) are known to be susceptible to two blood disorders in their early years. Approximately 10% of infants with DS develop transient abnormal myelopoiesis (TAM), a myeloproliferative disorder with an increase in leukocytes and blasts in peripheral blood [1, 2]. While most patients experience spontaneous remission within 6 months, about 10% of patients will have fatal liver dysfunction due to blastic infiltration [1, 3-6] and another 10-20% of patients develop Down syndrome-associated acute megakaryocytic leukemia (DS-AMKL) within 5 years [1, 3, 5, 7-9]. Meta-analyses of clinical reports of TAM and DS-AMKL [7, 10-14] and a case report of monozygotic twins [2, 13, 15, 16] have shown that almost all TAM and DS-AMKL cases have somatic mutations of *GATA-binding protein 1 (GATA1)* gene and that these mutations are essential in the multi-step development process of DS-AMKL.

GATA1 is a representative hematopoietic transcription factor involved in early hematopoiesis and erythro-megakaryocytic cell development [17-27]. Various mutations in exons 2 to 3 of *GATA1* result in the loss of the full-length protein (GATA1fl) and the production of only the short-form protein (GATA1s) translated from the second ATG site, which lacks the amino-terminal activation domain [10, 28]. This means that, regardless of the pattern of the mutation, the resulting protein is always a single alternative form produced even without the mutation, albeit in small amounts. This distinguishes this

74 mutation from other oncogenic mutations.

75 Despite the obvious necessity for GATA1 mutations in trisomy-21 cells, the quantitative impact of
76 GATA1s protein produced as a result of the mutations has not been fully elucidated. Indeed, although
77 some meta-clinical analyses have shown a significant association between the GATA1s expression
78 levels predicted from the variants and the severity of TAM and the frequency of AMKL [29], the early
79 stage pathogenesis is not fully understood. In particular, it remains unclear whether there is a direct
80 causal relationship beyond correlation between the amount of GATA1s protein, rather than its presence
81 per se, and early hematopoietic cell fate associated with disease-specific blood findings.

82 An in vitro model using PSCs was reported to be useful for analyzing diseases of early hematopoiesis
83 [31-33]. Of course, it is hard to precisely address if the level of gene expressions in PSC-derived
84 hematopoietic cells be the same in cells of comparable stages in primary disease development during
85 fetal hematopoiesis, but several PSC models of TAM have been already reported to recapitulate a
86 differentiation preference for myelocytes due to *GATA1* mutations and an increase in $CD34^+$ immature
87 megakaryoblasts associated with expression level of GATA1s [34-36] , which correspond to the
88 features observed in patients. Furthermore, recent study using trisomy-21 PSCs identified an
89 $CD34^+CD43^+CD11b^-CD71^+CD41^+CD235a^-$ megakaryocytic progenitor population largely
90 responsible for the myeloid proliferation in the absence of GATA1fl [37]. Interestingly, despite being
91 an erythro-megakaryocytic progenitor population, cells in this fraction possessed an expression profile

92 that showed a tendency for myeloid differentiation, which suggested the need for a more detailed
93 analysis of the effect of GATA1s on the nature of progenitors in earlier developmental stages. Current
94 study therefore examined the effects of higher or lower amount of GATA1s protein levels on each
95 lineage cell by additionally induce GATA1s expression in early-stage hematopoietic cells derived from
96 *GATA1* mutant PSCs.
97

Materials and methods

Ethical statement

To establish and use induced pluripotent stem cells (iPSCs), written informed consent was obtained from the guardians of the DS patient (ID: CiRA12345 at Kyoto University and 778 at Hirosaki University) in accordance with the Declaration of Helsinki. The use of human embryonic stem cells (ESCs) in Kyoto University and Tottori University was approved by the Ministry of Education Culture, Sports, Science and Technology of Japan (MEXT). This study was approved by the Ethics Committee and the recombinant DNA Experiments Safely Committee of Kyoto University. All methods were performed in accordance with the relevant guidelines and regulations.

Cells and cell culture

The cell line Ts21-ES-*GATA1*-WT, in which a human chromosome 21 was transferred into the human ESC line, KhES-1-derived subline, and Ts21-ES-*GATA1s*, in which the GATA1 mutation was introduced into the KhES-1-derived subline and then a human chromosome 21 was transferred into the *GATA1s*-ES, were previously established [34]. TAM-iPS-*GATA1s*, which was generated from the blasts of TAM patients with DS, and TAM-iPS-*GATA1*-WT, in which the *GATA1* mutation of TAM-iPS-*GATA1s* was repaired, were established as described previously [37]. All PSCs were cultured on

116 0.25 μg/cm^2 Laminin511-E8 fragment iMatrix-511 silk (Nippi, Tokyo, Japan)-coated culture plates
117 with StemFit AK02 medium (Ajinomoto, Tokyo, Japan). For passage, the cells were dissociated into
118 single cells with 0.5×TrypLE Select (Thermo Fisher Scientific, Waltham, MA, USA) and plated at 265
119 cells/cm^2. 10 μM Rock inhibitor Y-27632 (Nacalai Tesque, Kyoto, Japan) was used at the time of the
120 plating, and the medium was exchanged with fresh AK02 medium without Y-27632 the next day.
121

122 Generation of stable Dox-inducible GATA1fl-HA and GATA1s-
123 HA cell lines

124 The *adeno-associated virus integration site 1* (*AAVS1*) targeting pAAVS1-Tet-on-hGATA1Δex2-HA
125 vector was generated by replacing the CRISPRi cassette of pAAVS1-NDi-CRISPRi (Gen2) purchased
126 from Addgene (plasmid #73498; http://n2t.net/addgene:73498; RRID:Addgene_73498) [38] with C-
127 terminal HA-tagged GATA1Δex2 amplified from the cDNA of the cell line K562 using an In-Fusion
128 HD Cloning Kit (Clontech, Mountain View, CA, USA). The neomycin resistant gene expression
129 cassette was replaced with the hygromycin resistant gene generated by DNA synthesis. The resulting
130 pAAVS1-Tet-on-hGATA1Δex2-HA vector and Cas9/gRNA expressing vector AAVS1 T2 CRISPR in
131 pX330 purchased from Addgene (plasmid #72833; http://n2t.net/addgene:72833;
132 RRID:Addgene_72833) [39] were electroporated into Ts21-ES clones using a NEPA21 electroporator
133 (NEPAGENE, Chiba, Japan). Transfected cells were selected with 50 μg/mL hygromycin (InvivoGen,

San Diego, CA, USA). Hygromycin-resistant clones were picked, and successful targeting was confirmed by Sanger sequencing. To generate PB-Tet-on-hGATA1fl-HA vector, the second ATG of the C-terminal HA-tagged GATA1fl fragment amplified from the cDNA of K562 cells was replaced with CTC and cloned into an all-in-one PiggyBac-based Tet-inducible expression cassette vector synthesized in our laboratory. PB-Tet-on-hGATA1-HA vector and PiggyBac transposase vector were electroporated into Ts21-ES-*GATA1s* using the NEPA21 electroporator. Transfected cells were selected with 0.5 - 1 μg/mL puromycin (InvivoGen).

Hematopoietic differentiation

The hematopoietic differentiation was performed as previously described (**Fig 1B**) [40, 41]. In brief, undifferentiated PSC colonies were prepared on Laminin511-E8 fragment-coated culture plates with StemFit AK02 medium by seeding single cells or spheroids. When individual colonies reached 750 to 1000 μm in diameter, the culture medium was replaced with Essential 8 medium (Thermo Fisher Scientific) containing 80 ng/mL BMP4 (R&D Systems, Minneapolis, MN, USA), 80 ng/mL VEGF (R&D Systems) and 2 μM GSK-3 inhibitor CHIR99021 (Merck Millipore, Burlington, MA, USA). The cells were cultured at 37 ℃, 5% CO2 and 5% O2 during differentiation. On day 2, the medium was replaced with Essential 6 medium (Thermo Fisher Scientific) containing 25 ng/mL bFGF (Wako, Osaka, Japan), 80 ng/mL VEGF, 50 ng/mL SCF (R&D Systems) and 2 μM SB431542 (Sigma-Aldrich,

St. Louis, MO, USA). On day 4, the medium was replaced with Stemline® Ⅱ medium (Sigma-Aldrich) containing 80 ng/mL VEGF, 50 ng/mL SCF, 50 ng/mL Flt-3 Ligand (R&D Systems), 50 ng/mL IL-3 (R&D Systems), 50 ng/mL IL-6 (R&D Systems) and 5 ng/mL thrombopoietin (TPO, R&D Systems). On day 6, the cultured cells were gently dissociated with 0.5×TrypLE Select and filtered through a 40 μm cell strainer. Hematopoietic progenitor cells (HPCs) sorted by FACS Aria Ⅱ (BD Biosciences, San Jose, CA, USA) were cultured at a density of 1×10^4 cells per well in 24-well plate with Stemline® Ⅱ medium containing 50 ng/mL SCF, 50 ng/mL Flt-3 Ligand, 50 ng/mL IL-3, 50 ng/mL IL-6, 5 ng/mL TPO and 2 U/mL erythropoietin (EPO, Merck Millipore). The same amount of medium was added every 2 days, and the cells were re-seeded at a density of 2×10^4 cells per well in a 24-well plate on day 9 and day 12.

Cell sorting and flow cytometric analyses

The isolation of HPCs on day 6 and subsequent flow cytometric analysis were performed by using a FACS Aria Ⅱ (BD Biosciences). The antibodies used are described in **Table 1**. Collected cells were counted using C-chip (NanoEnTek, Seoul, Korea) or Countess® Ⅱ FL automated cell counter (Thermo Fisher Scientific) and stained in PBS containing 2% FBS for 20 minutes on ice. Samples were analyzed using FlowJo software (FlowJo LLC, Ashland, OR, USA).

Table 1. Antibodies used for flow cytometric analysis.

Antigen	Fluorochrome	Clone	Clonality	Source	Catalog #
CD309 (KDR)	Alexa Fluor® 647	7D4-6	monoclonal	Biolegend	359910
CD235a	BV421	GA-R2 (HIR2)	monoclonal	BD Biosciences	562938
CD34	Brilliant Violet 605	581	monoclonal	Biolegend	343529
CD43	PE/Cy7	CD43-10G7	monoclonal	Biolegend	343208
CD45	FITC	2D1	monoclonal	Biolegend	368508
CD42b	PE	HIP1	monoclonal	Biolegend	303906
CD71	APC	CY1G4	monoclonal	Biolegend	334108
CD33	PE/Cy7	WM53	monoclonal	Biolegend	303434
CD41	APC/Cy7	HIP8	monoclonal	Biolegend	303716
CD11b	PerCP/Cy5.5	ICRF44	monoclonal	Biolegend	301328

(Biolegend, San Diego, CA, USA)

List of antibodies used for flow cytometric analysis.

Immunoblotting

To confirm the expression of Dox-inducible GATA1 protein, protein was extracted from human PSCs

176 treated with or without 1 μg/mL Dox for 24 hours with RIPA buffer (Wako) supplemented with 2%
177 protease inhibitor cocktail (Nacalai, Kyoto, Japan). Each sample was separated by 10% sodium
178 dodecyl sulfate polyacrylamide gel electrophoresis and transferred to PVDF membranes (Merck
179 Millipore). The membrane was blocked with 5% dry milk and incubated with an anti-GATA1 primary
180 antibody (CST #4589, 1/1,000, Danvers, MA, USA) overnight at 4 ℃. The membrane was then
181 incubated with anti-rabbit IgG, HRP-linked secondary antibody (CST #7074, 1/5,000) for 1 hour at
182 room temperature. To confirm the amount of loaded protein, the membrane was stripped with WB
183 stripping solution strong (Nacalai) and probed with β-actin (13E5) rabbit mAb (CST #4970, 1/2,000).
184 Signals were detected with Chemi-Lumi One Super (Nacalai) and scanned with ImageQuant LAS
185 4000 (GE Healthcare, Chicago, IL, USA).
186

187 # Statistical analyses

188 Statistical analyses were performed with GraphPad Prism 6 (GraphPad Soft, La Jolla, CA, USA).
189 Results are shown as the mean ± SD and compared with the unpaired Student's *t*-test.
190

Results

$CD235a^{-}CD34^{+}CD43^{+}$ early-phase multipotent progenitors recapitulate the hematopoietic features of TAM

In order to precisely analyze the effect of *GATA1* genotype on the hematopoietic differentiation process, we prepared two sets of isogenic PSC pairs with trisomy of chromosome 21. One pair was human ESCs transferred chromosome 21 (Ts21-ES-*GATA1*-WT) and the same line with *GATA1* mutation introduced (Ts21-ES-*GATA1s*) [34]. The other pair was iPSCs (TAM-iPS-*GATA1s*) established from the blasts of a TAM patient with DS and with the *GATA1* mutation that repaired (TAM-iPS-*GATA1*-WT) [37] (**Fig 1A**). To compare these isogenic pairs, we conducted hematopoietic differentiation (**Fig 1B**).

Fig 1. $CD235a^{-}CD34^{+}CD43^{+}$ early-phase multipotent progenitors recapitulate the hematopoietic features of TAM.

(A) Scheme of the *GATA1*-WT and *GATA1s* Ts21-PSC isogenic pairs used in this study. (B) Schematic method for hematopoietic differentiation. $CD235a^{+}CD34^{+}CD43^{+}$ cells or $CD235a^{-}CD34^{+}CD43^{+}$ cells (HPCs) were sorted on day 6 and transferred to suspension culture. HPCs were continuously cultured,

209 and cell count and flow cytometry were performed on day 9, day 12 and day 16. (C, E) Representative
210 flow cytometry results and counts of each lineage on day 16 differentiated from the CD235a$^-$
211 CD34$^+$CD43$^+$ population of day 6 (C) Ts21-ES clones and (E) TAM-iPS clones. (D, F) Changes in the
212 number of immature myeloid cells differentiated from the CD235a$^-$CD34$^+$CD43$^+$ population of day 6
213 (D) Ts21-ES clones and (F) TAM-iPS clones (n = 5 biologically independent experiments for Ts21-
214 ES, n = 4 for TAM-iPS-*GATA1*-WT, n = 3 for TAM-iPS-*GATA1s*). Data are presented as the mean ±
215 SD. *$p < 0.05$, **$p < 0.01$, ***$p < 0.001$, ****$p < 0.0001$ by two-tailed unpaired Student's *t*-test for
216 myeloid lineages. Ery, erythrocytic cells; Meg, megakaryocytic cells; Mye, myeloid cells.
217
218 In our hematopoietic differentiation system, KDR$^-$CD34$^+$CD43$^+$ early-phase HPCs arose from both
219 *GATA1*-WT and *GATA1s* strains on day 6 of the initial differentiation and were divided into two
220 fractions: CD235a positive and negative, respectively (**S1A Fig**). From the early period of the
221 secondary culture after sorting, CD235a$^+$ HPCs in the *GATA1*-WT strains already showed commitment
222 to erythroid (CD235a$^+$CD42b$^-$) cells on day 9 (**S1B-S1C and S1E-S1F Figs**) and almost no production
223 of immature myeloid cells (CD34$^+$CD235a$^-$CD41$^-$CD42b$^-$CD45$^+$) (**S1D and S1G Figs**). In contrast,
224 CD235a$^-$ HPCs produced immature myeloid cells (**S1D and S1G Figs**) and finally differentiated into
225 all erythroid, megakaryocytic (CD235a$^-$CD41$^+$) and myeloid (CD235a$^-$CD41$^-$CD42b$^-$CD45$^+$) lineage
226 cells on day 16 (**Figs 1C and 1E**), which suggested the multipotency of the later subpopulation in our

hematopoietic system. To dissect the spatiotemporal impact of *GATA1* mutation on each lineage cell fate, we applied the $KDR^{-}CD235a^{-}CD34^{+}CD43^{+}$ fraction to subsequent cultures as early-phase multipotent HPCs (hereafter called "early HPCs").

Compared to the *GATA1*-WT strains, early HPCs in *GATA1s* strains produced few erythroid lineage cells and much more myeloid lineage cells (**Figs 1C and 1E**). Of note, while immature myeloid cells derived from the *GATA1*-WT strains continued to decrease with time, those from the *GATA1s* strains increased until day12 of the culture and were maintained significantly longer than in the *GATA1*-WT strains thereafter (**Figs 1D and 1F**). Both strains gave rise to megakaryocytic lineage cells (**Figs 1C and 1E**), which is consistent with previous studies that showed GATA1fl is not essential for specification into megakaryocytes, unlike erythrocytes [22, 30, 34-36, 42]. Taken together, these data indicated that early HPCs can recapitulate the hematopoietic features of TAM [1].

Establishment of Doxycycline-inducible GATA1s- or GATA1fl-expressing clones

Previous studies have reported that GATA1s is not just the cause of increased myelocytes in TAM, but also that higher expression levels correlate with severe disease groups [29, 30]. On the other hand, the incidence of DS-AMKL, which is an oncogenic blast proliferation derived from megakaryocytic

245 progenitors, correlates with a lower expression of GATA1s, suggesting that GATA1s has different
246 effects on the myeloid and megakaryocytic lineages in the absence of GATA1fl [7, 29]. To clarify this
247 spatiotemporal quantitative effect of GATA1s protein on the nature of multipotent progenitors and
248 each lineage cell type, we next analyzed the differentiation properties of *GATA1s* strains introduced
249 with Dox-inducible GATA1s expression cassettes (**Fig 2A and S2A-S2B Figs**). Additionally, we
250 generated *GATA1*-WT strains with Dox-inducible GATA1s expression cassettes and *GATA1s* strains
251 in which we added the Dox-inducible GATA1fl expression cassettes to evaluate the emergence and
252 rescue of disease phenotypes, respectively (**S2C Fig and Fig 2B**). The insertion of the GATA1s
253 expression cassette was confirmed by genomic PCR (**S2B Fig**), and protein expressions induced by
254 Dox treatment were confirmed by western blotting analyses (**Fig 2C**). Karyotypes of each clones was
255 confirmed by Q-banding analysis (**S3A-S3E Figs**). To confirm whether there is reproducibility beyond
256 the clones, we also generated corresponding subclones in TAM-iPS clones (**S4A Fig**), and confirmed
257 karyotypes and Dox-inducible expression of GATA1 protein (**S4B-S4G Figs**).
258
259 **Fig 2. Establishment of Dox-inducible GATA1s or GATA1fl Ts21-ES cells.**
260 (A) Scheme of the Dox-inducible GATA1s. (B) Parental clones and generated GATA1s or GATA1fl
261 Dox-inducible subclones. The Dox-inducible GATA1s construct was knocked into *AAVS1* locus with
262 the CRISPR-Cas9 system, and the Dox-inducible GATA1fl construct was transduced by the PiggyBac

system. (C) Western blot analysis of GATA1s and GATA1fl expression in untreated ESCs and ESCs treated with 1 μg/ml Dox for 24 h. K562 was used as the positive control.

GATA1s protein acts to quantitatively sustain immature myeloid cells in competition with GATA1fl

Using the series of modified cells, we examined the quantitative effects of GATA1s by lineage. GATA1s overexpression in early HPCs on day 6 significantly increased commitment into myeloid lineage (**Figs 3A and 3B**). Moreover, overexpression from day 9 of the differentiation, when immature myeloid progenitors had already appeared in culture (**Fig 1D**), also significantly increased the number of immature myeloid progenitors (**Figs 3C and 3D**). Considering that GATA1fl deficiency itself led to an increase in myeloid cells even without exogenous *GATA1s* expression (**Fig 1D**), these results suggested that GATA1s leads to a further proliferation of the myeloid lineage brought about by the loss of GATA1fl by sustaining committed progenitors. Consistent with this result, we observed that overexpression of GATA1s tended to increase the number of colonies containing non-megakaryocytic (non-Mk) cells in colony-forming unit assay of megakaryocytic progenitors (CFU-Mk) (**S5A-S5B and S5D Figs**) and larger non-Mk colonies was seen in GATA1s overexpressed samples (**S5E Fig**) as previously reported [30]. In TAM-iPS-*GATA1s* derived clones, due to differences in the differentiation

281 properties, it was not possible to detect increase myeloid commitment by quantitative increase of
282 GATA1s (**S6A and S6B Figs**), but there was tendency toward enhanced maintenance of immature
283 myeloid cells (**S6C and S6D Figs**). These results are consistent with the exacerbation of
284 myeloproliferation in patients with a higher expression of GATA1s. Similar results were obtained in
285 *GATA1*-WT strains introduced with *GATA1s* (**S7A and S7B Figs**) and similar result was obtained for
286 TAM-iPS-*GATA1*-WT derived clone (**S8A and S8B Figs**). Whereas, the opposite was observed in
287 *GATA1s* strains that overexpressed GATA1fl (**Figs 3C and 3D**), demonstrating that GATA1s and
288 GATA1fl competitively increase and decrease myeloid lineages.
289
290 **Fig 3. Quantitative increase of GATA1s in early-phase increases myeloid commitment and**
291 **enhances the maintenance of immature myeloid cells.**
292 (A) Representative flow cytometry of staining for CD34 and CD45 among myeloid cells on day 9.
293 Upper panels indicate the Dox-untreated sample and lower panels indicate the Dox-treated sample
294 from day 6 for each clone. (B) Fold changes of immature myeloid cells over each untreated sample on
295 day 9. (C) Representative flow cytometry of staining for CD34 and CD45 among myeloid cells on day
296 16 with or without Dox treatment from day 9. (D) Fold changes of immature myeloid cells over each
297 untreated sample on day 16 (n = 5 biologically independent experiments for Ts21-s and Ts21-s-Δex2,

298 n = 3 for Ts21-s-fl). Data are presented as the mean ± SD. *$p < 0.05$, **$p < 0.01$ vs. Ts21-s under the
299 same treatment by two-tailed unpaired Student's *t*-test.
300
301 # GATA1s protein has conflicting effects on megakaryocyte
302 # commitment and persistence in the absence of GATA1fl
303
304 Contrary to the correlation with myeloproliferation seen in TAM, meta-clinical analyses on the impact
305 of *GATA1* mutation in DS-AMKL are somewhat paradoxical. Although almost all DS-AMKL patients
306 have a *GATA1* mutation, some studies have shown that an increased expression of GATA1s is inversely
307 associated with the risk of DS-AMKL [29]. We therefore evaluated the spatiotemporal effects of
308 GATA1s on megakaryocytic lineage, a potential origin of DS-AMKL, following differentiation.
309 GATA1s overexpression in early HPCs significantly reduced megakaryocytic commitment in *GATA1s*
310 strains (**Figs 4A and 4B**). Similar results was obtained with TAM-iPS-*GATA1s* derived clone (**S9A**
311 **and S9B Figs**). Consistent with this result, we observed that the overexpression of GATA1s
312 significantly reduced the total number of CFU-Mk (**S5A-S5C Figs**). Furthermore, an effect of
313 GATA1s overexpression was observed in *GATA1s* strains but not in *GATA1*-WT strains (**S7C and S7D**
314 **Figs**) and in TAM-iPS-*GATA1*-WT derived clone (**S8C and S8D Figs**), suggesting that the effects on
315 megakaryocytic lineage are counteracted by endogenous GATA1fl, even at high concentrations of

316 GATA1s. On the other hand, unexpectedly, GATA1fl overexpression did not restore the
317 megakaryocytic differentiation of *GATA1s* strains, but rather reduced it as in the case of GATA1s
318 overexpression (**S10A-S10B and S11A-S11B Figs**). Because the predominant restoration of erythroid
319 differentiation was observed at this time (**S10C-S10E and S11C-S11E Figs**), these results indicated
320 that GATA1fl at the endogenous expression level is important for the commitment to both erythroid
321 and megakaryocytic lineages, but a higher expression at this stage leads to a significant bias towards
322 erythroid commitment due to its essential role in erythropoiesis, which consequently suppresses
323 megakaryocyte commitment.
324
325 **Fig 4. Quantitative increase of GATA1s in early-phase suppresses megakaryocytic**
326 **differentiation and in later-phase increases the persistence of immature megakaryocytic cells.**
327 (A) Representative flow cytometry of staining for CD34 and CD41 on day 9. Upper panels indicate
328 the Dox-untreated sample and lower panels indicate the Dox-treated sample from day 6 for each clone.
329 (B) Fold changes of immature megakaryocytic cells over each untreated sample on day 9. (C)
330 Representative flow cytometry of staining for CD41 and CD42b on day 16 with or without Dox
331 treatment from day 12. (D) Fold changes of megakaryocytic cells over each untreated sample on day
332 16. (E) Representative flow cytometry of staining for CD34 and CD41 on day 16 with or without Dox
333 treatment from day 12. (F) Fold changes of immature megakaryocytic cells over each untreated sample

on day 16 (n = 5 biologically independent experiments for Ts21-s and Ts21-s-Δex2, n = 3 for Ts21-s-fl). Data are presented as the mean ± SD. *$p < 0.05$, ***$p < 0.001$, ****$p < 0.0001$ vs. Ts21-s under the same treatment by two-tailed unpaired Student's *t*-test.

The inhibitory effects of GATA1s on megakaryocytic commitment could explain the lower risk of DS-AMKL progression in cases of high GATA1s expression among TAM patients [29]. Nevertheless, it is still clinically evident that *GATA1* mutations are by far the most important risk factor for developing DS-AMKL, even in patients with a high expression of GATA1s [1, 2]. These facts led us to examine if there is another cause of the accumulation of immature megakaryocytes that could be responsible for DS-AMKL even in GATA1s high-expressing cells with suppressed commitment. Indeed, we found the overexpression of either GATA1s and GATA1fl significantly increased the percentage of total megakaryocytes in *GATA1s* strains after day 12 of the differentiation (**Figs 4C and 4D**)**.** However, when focusing on immature megakaryocytic progenitor cells, GATA1s overexpression had a significantly increased $CD34^+CD41^+$ subpopulation, but GATA1fl overexpression did not. (**Figs 4E and 4F**). In TAM-iPS-*GATA1s* derived clone, although there was no significant difference in total megakaryocytes, there was a trend toward an increase (**S9C-S9D Figs**). Whereas, when we focused on immature megakaryocytic cells, we found that the overexpression of GATA1s in megakaryocytic progenitors on later stage significantly increased the persistence of immature megakaryocytic cells,

but GATA1fl overexpression did not (**S9E-S9F Figs**). These results indicated that GATA1s works to maintain immature cells in megakaryocytic lineage as well as myeloid lineage, but unlike the myeloid lineage, the overexpression of GATA1s in the *GATA1*-WT strain did not have any effect on immature megakaryocytic cells (**S7E-S7F and S8E-S8F Figs**). Therefore, the effects of higher GATA1s expression on the maintenance of mutant strain-derived megakaryocytic progenitors are dependent on differences in the responsiveness of the target cells to GATA1s protein, which are conferred by the mutation itself.

Discussion

The exclusive expression of GATA1s protein as a result of *GATA1* mutations is an essential process for the onset of both TAM and DS-AMKL. Even though blasts in patients in most cases have been found to be a heterogeneous population with a variety of *GATA1* mutations at different expression levels, no study has experimentally examined how the intensity of the gene expression contributes to the pathologies of both diseases. Focusing on this point, we clarified how the spatiotemporal shift of GATA1s protein expression affects the progenitor cells from which both diseases originate by using a PSC model and stepwise hematopoietic differentiation. We successfully observed the quantitative impact of the GATA1s expression level on each stage of each lineage by utilizing a Dox-inducible expression system.

PSC-based studies can reveal new effects of mutant genes that cannot be elucidated by studies using patient primary cells after the disease onset or cell lines that are already addicted to the mutations themselves. Moreover, with respect to DS, there is no suitable mouse model that replicates the phenotypes of human trisomy-21. While previous studies including the over-expression of GATA1s in fetal liver progenitor cells of *Gata1*$^{\Delta N}$ mice and cord blood CD34^{+} hematopoietic progenitor cells have reported the GATA1s-dependent expansion of *GATA1* mutant cells in myeloid and megakaryocytic lineages [30, 43], our study distinguished the effects of GATA1s on the commitment and proliferation

of the myeloid and megakaryocytic lineages in the absence of GATA1fl by focusing on the progenitor cells which correspond to common myeloid progenitors, originally defined as an origin of both granulocyte/macrophage progenitors and megakaryocyte/erythrocyte progenitors. Specifically, we found that commitment to megakaryocytes at the early HPC stage were significantly reduced by elevated GATA1s expression, and only in the absence of GATA1fl were the megakaryocyte progenitors maintained in response to GATA1s expression levels. These mutation- and differentiation stage-specific reversal effects contrasted the results regarding myeloid lineage, where GATA1s simply sustained and increased progenitor cells in competition with GATA1fl.

Two hypotheses may explain why once committed megakaryocytic progenitors acquire the ability to proliferate in response to GATA1s like myeloid progenitors only under conditions without GATA1fl. First, some additional genetic or epigenetic modifications that occur during tumorigenesis might confer GATA1s-responsive growth characteristics. Alternatively, GATA1fl deficiency itself might provide intracellular signaling for the perturbation. Indeed, a previous study using trisomy-21 PSCs revealed that the expression profile of a GATA1fl-deficient megakaryocytic progenitor subpopulation responsible for myeloproliferation was biased toward the myeloid lineage [37]. Therefore, GATA1s could hijack the myeloid mechanism to promote the proliferation of megakaryocytic progenitors. Further study of this hypothesis using methods that directly examine access of the GATA1 protein to genomic DNA, such as electrophoretic mobility shift assays and chromatin immunoprecipitation, are

needed. Such studies could also reveal new molecular mechanisms, by which the higher expression of GATA1s suppresses megakaryocytic commitment in early HPCs.

Collectively, our results suggested that although *GATA1* mutant cells cause the increase in myeloid and megakaryocytic progenitors regardless of the intensity of GATA1s expression, the pathways vary with their expression levels **(Fig 5)**. This model provides an explanation for the paradoxical clinical features in which higher and lower GATA1s expressions are inversely correlated with the severity of TAM and development of DS-AMKL among patients with TAM even though *GATA1* mutations are the definitive etiology of both diseases. Future in vitro and in vivo studies are expected to provide more definitive evidence for this model.

Fig 5. Graphical abstract of *GATA1*-WT, *GATA1s* and the effects of GATA1s overexpression on *GATA1s* strain.

With wild-type *GATA1* (*GATA1*-WT), which expresses both the full length (GATA1fl) and short form (GATA1s) of GATA1 protein, all erythrocytic (Ery), megakaryocytic (Meg) and myeloid (Mye) lineages are produced. In the case of *GATA1s* mutation, erythroid differentiation is markedly impaired and myeloid cells are increased. With the additional overexpression of GATA1s, *GATA1s* mutation suppresses megakaryocytic differentiation and increases myeloid commitment. In addition, the persistence of immature megakaryocytic cells is enhanced in the later phase.

414

Acknowledgements

We thank Ms. Harumi Watanabe for providing administrative assistance, Dr. Peter Karagiannis for proofreading the paper, and Prof. Tsutomu Toki and Prof. Etsuro Ito (Hirosaki University) for obtaining informed consent from the patient and harvesting primary cells for the establishment of iPSCs.

References

1. Massey GV, Zipursky A, Chang MN, Doyle JJ, Nasim S, Taub JW, et al. A prospective study of the natural history of transient leukemia (TL) in neonates with Down syndrome (DS): Children's Oncology Group (COG) study POG-9481. Blood. 2006;107(12):4606-13. doi: 10.1182/blood-2005-06-2448. PubMed PMID: 16469874.

2. Pine SR, Guo Q, Yin C, Jayabose S, Druschel CM, Sandoval C. Incidence and clinical implications of GATA1 mutations in newborns with Down syndrome. Blood. 2007;110(6):2128-31. doi: 10.1182/blood-2007-01-069542. PubMed PMID: 17576817.

3. Klusmann JH, Creutzig U, Zimmermann M, Dworzak M, Jorch N, Langebrake C, et al. Treatment and prognostic impact of transient leukemia in neonates with Down syndrome. Blood. 2008;111(6):2991-8. doi: 10.1182/blood-2007-10-118810. PubMed PMID: 18182574; PubMed Central PMCID: PMCPMC2265448.

4. Muramatsu H, Kato K, Watanabe N, Matsumoto K, Nakamura T, Horikoshi Y, et al. Risk factors for early death in neonates with Down syndrome and transient leukaemia. British journal of haematology. 2008;142(4):610-5. doi: 10.1111/j.1365-2141.2008.07231.x. PubMed PMID: 18510680.

5. Gamis AS, Alonzo TA, Gerbing RB, Hilden JM, Sorrell AD, Sharma M, et al. Natural

history of transient myeloproliferative disorder clinically diagnosed in Down syndrome neonates: a report from the Children's Oncology Group Study A2971. Blood. 2011;118(26):6752-9. doi: 10.1182/blood-2011-04-350017. PubMed PMID: WOS:000298401000011.

6. Bhatnagar N, Nizery L, Tunstall O, Vyas P, Roberts I. Transient Abnormal Myelopoiesis and AML in Down Syndrome: an Update. Current hematologic malignancy reports. 2016;11(5):333-41. doi: 10.1007/s11899-016-0338-x. PubMed PMID: 27510823; PubMed Central PMCID: PMCPMC5031718.

7. Yoshida K, Toki T, Okuno Y, Kanezaki R, Shiraishi Y, Sato-Otsubo A, et al. The landscape of somatic mutations in Down syndrome-related myeloid disorders. Nature genetics. 2013;45(11):1293-9. doi: 10.1038/ng.2759. PubMed PMID: 24056718.

8. Roberts I, Alford K, Hall G, Juban G, Richmond H, Norton A, et al. GATA1-mutant clones are frequent and often unsuspected in babies with Down syndrome: identification of a population at risk of leukemia. Blood. 2013;122(24):3908-17. doi: 10.1182/blood-2013-07-515148. PubMed PMID: 24021668; PubMed Central PMCID: PMCPMC3995281.

9. Roy A, Roberts I, Norton A, Vyas P. Acute megakaryoblastic leukaemia (AMKL) and transient myeloproliferative disorder (TMD) in Down syndrome: a multi-step model

of myeloid leukaemogenesis. British journal of haematology. 2009;147(1):3-12. doi: 10.1111/j.1365-2141.2009.07789.x. PubMed PMID: 19594743.

10. Wechsler J, Greene M, McDevitt MA, Anastasi J, Karp JE, Le Beau MM, et al. Acquired mutations in GATA1 in the megakaryoblastic leukemia of Down syndrome. Nature genetics. 2002;32(1):148-52. doi: 10.1038/ng955. PubMed PMID: 12172547.

11. Mundschau G, Gurbuxani S, Gamis AS, Greene ME, Arceci RJ, Crispino JD. Mutagenesis of GATA1 is an initiating event in Down syndrome leukemogenesis. Blood. 2003;101(11):4298-300. doi: 10.1182/blood-2002-12-3904. PubMed PMID: 12560215.

12. Hitzler JK, Cheung J, Li Y, Scherer SW, Zipursky A. GATA1 mutations in transient leukemia and acute megakaryoblastic leukemia of Down syndrome. Blood. 2003;101(11):4301-4. doi: 10.1182/blood-2003-01-0013. PubMed PMID: 12586620.

13. Rainis L, Bercovich D, Strehl S, Teigler-Schlegel A, Stark B, Trka J, et al. Mutations in exon 2 of GATA1 are early events in megakaryocytic malignancies associated with trisomy 21. Blood. 2003;102(3):981-6. doi: 10.1182/blood-2002-11-3599. PubMed PMID: 12649131.

14. Ahmed M, Sternberg A, Hall G, Thomas A, Smith O, O'Marcaigh A, et al. Natural history of GATA1 mutations in Down syndrome. Blood. 2004;103(7):2480-9. doi:

474 10.1182/blood-2003-10-3383. PubMed PMID: 14656875.

475 15. Stark B, Jeison M, Preudhomme C, Fenaux P, Ash S, Korek Y, et al. Acquired trisomy
476 21 and distinct clonal evolution in acute megakaryoblastic leukaemia in young
477 monozygotic twins. British journal of haematology. 2002;118(4):1082-6. doi:
478 10.1046/j.1365-2141.2002.03756.x. PubMed PMID: 12199789.

479 16. Shimada A, Xu G, Toki T, Kimura H, Hayashi Y, Ito E. Fetal origin of the GATA1
480 mutation in identical twins with transient myeloproliferative disorder and acute
481 megakaryoblastic leukemia accompanying Down syndrome. Blood. 2004;103(1):366.
482 doi: 10.1182/blood-2003-09-3219. PubMed PMID: 14684662.

483 17. Martin DI, Zon LI, Mutter G, Orkin SH. Expression of an erythroid transcription
484 factor in megakaryocytic and mast cell lineages. Nature. 1990;344(6265):444-7. doi:
485 10.1038/344444a0. PubMed PMID: 2320112.

486 18. Romeo PH, Prandini MH, Joulin V, Mignotte V, Prenant M, Vainchenker W, et al.
487 Megakaryocytic and erythrocytic lineages share specific transcription factors. Nature.
488 1990;344(6265):447-9. doi: 10.1038/344447a0. PubMed PMID: 2320113.

489 19. Martin DI, Orkin SH. Transcriptional activation and DNA binding by the erythroid
490 factor GF-1/NF-E1/Eryf 1. Genes & development. 1990;4(11):1886-98. doi:
491 10.1101/gad.4.11.1886. PubMed PMID: 2276623.

20. Pevny L, Simon MC, Robertson E, Klein WH, Tsai SF, D'Agati V, et al. Erythroid differentiation in chimaeric mice blocked by a targeted mutation in the gene for transcription factor GATA-1. Nature. 1991;349(6306):257-60. doi: 10.1038/349257a0. PubMed PMID: 1987478.

21. Orkin SH. GATA-binding transcription factors in hematopoietic cells. Blood. 1992;80(3):575-81. PubMed PMID: 1638017.

22. Visvader JE, Crossley M, Hill J, Orkin SH, Adams JM. The C-terminal zinc finger of GATA-1 or GATA-2 is sufficient to induce megakaryocytic differentiation of an early myeloid cell line. Mol Cell Biol. 1995;15(2):634-41. doi: 10.1128/mcb.15.2.634. PubMed PMID: 7823932; PubMed Central PMCID: PMCPMC231921.

23. Weiss MJ, Orkin SH. Transcription factor GATA-1 permits survival and maturation of erythroid precursors by preventing apoptosis. Proceedings of the National Academy of Sciences of the United States of America. 1995;92(21):9623-7. doi: 10.1073/pnas.92.21.9623. PubMed PMID: 7568185; PubMed Central PMCID: PMCPMC40854.

24. Fujiwara Y, Browne CP, Cunniff K, Goff SC, Orkin SH. Arrested development of embryonic red cell precursors in mouse embryos lacking transcription factor GATA-1. Proceedings of the National Academy of Sciences of the United States of America.

510 1996;93(22):12355-8. doi: 10.1073/pnas.93.22.12355. PubMed PMID: 8901585;
511 PubMed Central PMCID: PMCPMC37995.
512 25. Shivdasani RA, Fujiwara Y, McDevitt MA, Orkin SH. A lineage-selective knockout
513 establishes the critical role of transcription factor GATA-1 in megakaryocyte growth
514 and platelet development. EMBO J. 1997;16(13):3965-73. doi:
515 10.1093/emboj/16.13.3965. PubMed PMID: 9233806; PubMed Central PMCID:
516 PMCPMC1170020.
517 26. Vyas P, Ault K, Jackson CW, Orkin SH, Shivdasani RA. Consequences of GATA-1
518 deficiency in megakaryocytes and platelets. Blood. 1999;93(9):2867-75. PubMed
519 PMID: 10216081.
520 27. Shimizu R, Takahashi S, Ohneda K, Engel JD, Yamamoto M. In vivo requirements
521 for GATA-1 functional domains during primitive and definitive erythropoiesis. EMBO
522 J. 2001;20(18):5250-60. doi: 10.1093/emboj/20.18.5250. PubMed PMID: 11566888;
523 PubMed Central PMCID: PMCPMC125635.
524 28. Xu G, Nagano M, Kanezaki R, Toki T, Hayashi Y, Taketani T, et al. Frequent
525 mutations in the GATA-1 gene in the transient myeloproliferative disorder of Down
526 syndrome. Blood. 2003;102(8):2960-8. doi: 10.1182/blood-2003-02-0390. PubMed
527 PMID: 12816863.

528 29. Kanezaki R, Toki T, Terui K, Xu G, Wang R, Shimada A, et al. Down syndrome and
529 GATA1 mutations in transient abnormal myeloproliferative disorder: mutation
530 classes correlate with progression to myeloid leukemia. Blood. 2010;116(22):4631-8.
531 doi: 10.1182/blood-2010-05-282426. PubMed PMID: 20729467.
532 30. Li Z, Godinho FJ, Klusmann JH, Garriga-Canut M, Yu C, Orkin SH. Developmental
533 stage-selective effect of somatically mutated leukemogenic transcription factor
534 GATA1. Nature genetics. 2005;37(6):613-9. doi: 10.1038/ng1566. PubMed PMID:
535 15895080.
536 31. Suzuki NM, Niwa A, Yabe M, Hira A, Okada C, Amano N, et al. Pluripotent cell
537 models of fanconi anemia identify the early pathological defect in human
538 hemoangiogenic progenitors. Stem Cells Transl Med. 2015;4(4):333-8. doi:
539 10.5966/sctm.2013-0172. PubMed PMID: 25762002; PubMed Central PMCID:
540 PMCPMC4367500.
541 32. Doulatov S, Vo LT, Macari ER, Wahlster L, Kinney MA, Taylor AM, et al. Drug
542 discovery for Diamond-Blackfan anemia using reprogrammed hematopoietic
543 progenitors. Sci Transl Med. 2017;9(376). doi: 10.1126/scitranslmed.aah5645.
544 PubMed PMID: 28179501; PubMed Central PMCID: PMCPMC5501179.
545 33. Karagiannis P, Yamanaka S, Saito MK. Application of induced pluripotent stem cells

546 to primary immunodeficiency diseases. Exp Hematol. 2019;71:43-50. doi:
547 10.1016/j.exphem.2019.01.005. PubMed PMID: 30664903.
548 34. Kazuki Y, Yakura Y, Abe S, Osaki M, Kajitani N, Kazuki K, et al. Down syndrome-
549 associated haematopoiesis abnormalities created by chromosome transfer and
550 genome editing technologies. Scientific reports. 2014;4:6136. doi: 10.1038/srep06136.
551 PubMed PMID: 25159877; PubMed Central PMCID: PMCPMC4145315.
552 35. Byrska-Bishop M, VanDorn D, Campbell AE, Betensky M, Arca PR, Yao Y, et al.
553 Pluripotent stem cells reveal erythroid-specific activities of the GATA1 N-terminus.
554 The Journal of clinical investigation. 2015;125(3):993-1005. doi: 10.1172/JCI75714.
555 PubMed PMID: 25621499; PubMed Central PMCID: PMCPMC4362246.
556 36. Banno K, Omori S, Hirata K, Nawa N, Nakagawa N, Nishimura K, et al. Systematic
557 Cellular Disease Models Reveal Synergistic Interaction of Trisomy 21 and GATA1
558 Mutations in Hematopoietic Abnormalities. Cell reports. 2016;15(6):1228-41. doi:
559 10.1016/j.celrep.2016.04.031. PubMed PMID: 27134169.
560 37. Nishinaka-Arai Y, Niwa A, Matsuo S, Kazuki Y, Yakura Y, Hiroma T, et al. Down
561 syndrome-related transient abnormal myelopoiesis is attributed to a specific erythro-
562 megakaryocytic subpopulation with GATA1 mutation. Haematologica. 2020. doi:
563 10.3324/haematol.2019.242693. PubMed PMID: 32354872.

564 38. Mandegar MA, Huebsch N, Frolov EB, Shin E, Truong A, Olvera MP, et al. CRISPR
565 Interference Efficiently Induces Specific and Reversible Gene Silencing in Human
566 iPSCs. Cell stem cell. 2016;18(4):541-53. doi: 10.1016/j.stem.2016.01.022. PubMed
567 PMID: 26971820; PubMed Central PMCID: PMCPMC4830697.
568 39. Natsume T, Kiyomitsu T, Saga Y, Kanemaki MT. Rapid Protein Depletion in Human
569 Cells by Auxin-Inducible Degron Tagging with Short Homology Donors. Cell reports.
570 2016;15(1):210-8. doi: 10.1016/j.celrep.2016.03.001. PubMed PMID: 27052166.
571 40. Ohta R, Niwa A, Taniguchi Y, Suzuki NM, Toga J, Yagi E, et al. Laminin-guided
572 highly efficient endothelial commitment from human pluripotent stem cells.
573 Scientific reports. 2016;6:35680. doi: 10.1038/srep35680. PubMed PMID: 27804979;
574 PubMed Central PMCID: PMCPMC5090224.
575 41. Honda-Ozaki F, Terashima M, Niwa A, Saiki N, Kawasaki Y, Ito H, et al. Pluripotent
576 Stem Cell Model of Nakajo-Nishimura Syndrome Untangles Proinflammatory
577 Pathways Mediated by Oxidative Stress. Stem Cell Reports. 2018;10(6):1835-50. doi:
578 10.1016/j.stemcr.2018.04.004. PubMed PMID: 29731430; PubMed Central PMCID:
579 PMCPMC5989695.
580 42. Muntean AG, Crispino JD. Differential requirements for the activation domain and
581 FOG-interaction surface of GATA-1 in megakaryocyte gene expression and

development. Blood. 2005;106(4):1223-31. doi: 10.1182/blood-2005-02-0551. PubMed PMID: 15860665; PubMed Central PMCID: PMCPMC1895209.

43. Maroz A, Stachorski L, Emmrich S, Reinhardt K, Xu J, Shao Z, et al. GATA1s induces hyperproliferation of eosinophil precursors in Down syndrome transient leukemia. Leukemia. 2014;28(6):1259-70. doi: 10.1038/leu.2013.373. PubMed PMID: 24336126; PubMed Central PMCID: PMCPMC4047213.

Supporting information

Supplemental materials and methods

Karyotyping

For karyotyping, cultured PSCs were incubated with 0.4 μg/mL KaryoMAX™ Colcemid™ solution (Thermo Fisher Scientific) for 1 h. Dissociated cells were treated with hypotonic solution and fixed with carnoy solution. Karyotyping of fixed samples was requested to Trans Chromosomics Co., Ltd. (Tottori, Japan).

Colony-forming unit assay of megakaryocytic progenitors

Colony-forming unit assay of megakaryocytic progenitors (CFU-Mk) was performed with MegaCult™-C with cytokines (#04901, STEMCELL technologies, Vancouver, Canada). 2.5×10^3 sorted $CD235a^-CD34^+CD43^+$ cells on day 6 were plated in MegaCult™-C collagen based medium with or without 1 μg/mL Dox and cultured for 10 days. Staining for GPⅡb/Ⅲa antibody and scoring of CFU colonies were performed in accordance with the manufacturer's instructions.

S1 Fig. Characterization of $CD235a^+CD34^+CD43^+$ cells compared with $CD235a^-CD34^+CD43^+$

607 **cells.**

608 (A) Gating strategy used to sort CD235a$^+$CD34$^+$CD43$^+$ and CD235a$^-$CD34$^+$CD43$^+$ HPCs on day 6.

609 (B-C, E-F) Representative flow cytometric analysis and cell number of each population on day 9

610 compared with the CD235a$^+$CD34$^+$CD43$^+$ (235a$^+$) and CD235a$^-$CD34$^+$CD43$^+$ (235a$^-$) populations of

611 (B, C) Ts21-ES-*GATA1*-WT and (E, F) TAM-iPS-*GATA1*-WT. (D, G) Changes in the number of

612 immature myeloid cells compared with the CD235a$^+$CD34$^+$CD43$^+$ and CD235a$^-$CD34$^+$CD43$^+$

613 populations differentiated on day 6 of (D) Ts21-ES-*GATA1*-WT and (G) TAM-iPS-*GATA1*-WT (n = 3

614 biologically independent experiments for CD235a$^+$CD34$^+$CD43$^+$ of Ts21-ES-*GATA1*-WT and TAM-

615 iPS-*GATA1*-WT, n = 5 for CD235a$^-$CD34$^+$CD43$^+$ of Ts21-ES-*GATA1*-WT and n = 4 for CD235a$^-$

616 CD34$^+$CD43$^+$ of TAM-iPS-*GATA1*-WT). Data are presented as the mean ± SD. *$p < 0.05$, **$p < 0.01$,

617 ***$p < 0.001$ by two-tailed unpaired Student's *t*-test. Ery, erythrocytic cells; Meg, megakaryocytic

618 cells; Mye, myeloid cells.

619

620 **S2 Fig. Establishment of GATA1 isoform Dox-inducible clones.**

621 (A) Schematic overview of the *AAVS1* targeting strategy by CRISPR-Cas9 to generate Dox-inducible

622 GATA1s for Ts21-ES lines. (B) Genomic PCR to confirm the integration of the Dox-inducible

623 GATA1s cassette. Expected fragment size: integration of Dox-inducible GATA1Δex2-HA, 8510 bp;

624 no integration, 1956 bp. (C) Scheme of Dox-inducible GATA1fl and PiggyBac vector for Dox-

625 inducible GATA1fl. The second ATG was replaced with CTC to express only GATA1fl.

626

627 **S3 Fig. Karyotyping of parental Ts21-ES clones and Dox-inducible GATA1s or GATA1fl knock-**

628 **in subclones.**

629 (A-E) Representative Q-banding karyotypes of (A) Ts21-ES-*GATA1*-WT (Ts21-WT), (B) Ts21-ES-

630 *GATA1s* (Ts21-s), (C) Ts21-WT-Δex2, (D) Ts21-s-Δex2 and (E) Ts21-s-fl.

631

632 **S4 Fig. Establishment of Dox-inducible GATA1s or GATA1fl TAM-iPS cells.**

633 (A) Parental clones and generated GATA1s or GATA1fl Dox-inducible subclones. The Dox-inducible

634 GATAs construct was knocked into *AAVS1* locus with CRISPR-Cas9 system, and the Dox-inducible

635 GATA1fl construct was transduced by the PiggyBac system. (B-F) Representative Q-banding

636 karyotypes of (B) TAM-iPS-*GATA1*-WT (TAM-WT), (C) TAM-iPS-*GATA1s* (TAM-s), (D) TAM-WT-

637 Δex2, (E) TAM-s-Δex2 and (F) TAM-s-fl. (G) Western blot analysis of GATA1s and GATA1fl

638 expression in untreated iPSCs and iPSCs treated with 1 μg/mL Dox for 24 h. K562 was used as the

639 positive control.

640

641 **S5 Fig. CFU-Mk is significantly decreased by GATA1s overexpression in *GATA1s* strains.**

642 (A) Representative images of each types of colonies in colony-forming unit assay of megakaryocytic

643 progenitors. (B-D) Numbers of CFUs resulting from 2,500 $CD235a^{-}CD34^{+}CD43^{+}$ cells on day 6 with
644 or without Dox treatment, (B) total, (C) total of CFU-Mk and (D) total of mixed CFU-Mk/ non-Mk
645 and non-Mk (n = 3 biologically independent experiments for Ts21-WT and Ts21-s-Δex2 and n = 4 for
646 Ts21-s). (E) Representative images of non-Mk colonies observed in Dox-untreated and Dox-treated
647 Ts21-s-Δex2. Scale bars: 100 μm. Data are presented as the mean ± SD. $^{**}p < 0.01$ vs. untreated
648 sample of each clones by two-tailed unpaired Student's *t*-test.
649
650 **S6 Fig. Quantitative increase of GATA1s in TAM-iPS-*GATA1s* derived cells shows tendency to**
651 **enhance the sustain of immature myeloid cells.**
652 (A) Representative flow cytometry of staining for CD34 and CD45 among myeloid cells on day 9.
653 Upper panels indicate the Dox-untreated sample and lower panels indicate the Dox-treated sample
654 from day 6 for each clone. (B) Fold changes of immature myeloid cells over each untreated sample on
655 day 9. (C) Representative flow cytometry of staining for CD34 and CD45 among myeloid cells on day
656 12 with or without Dox treatment from day 9. (D) Fold changes of immature myeloid cells over each
657 untreated sample on day 16 (n = 3 biologically independent experiments). Data are presented as the
658 mean ± SD. ns vs. TAM-s under the same treatment by two-tailed unpaired Student's *t*-test.
659
660 **S7 Fig. Overexpression of GATA1s has little effect on immature megakaryocytic cells in the**

presence of GATA1fl.

(A) Representative flow cytometry of staining for CD34 and CD45 among myeloid cells on day 12. Upper panels indicate the Dox-untreated sample and lower panels indicate the Dox-treated sample from day 9. (B) The fold changes of immature myeloid cells over each untreated sample on day 12 and day 16. (C, E) Representative flow cytometry of staining for CD34 and CD41 (C) on day 9 with or without Dox treatment from day 6 and (E) on day 16 with or without Dox treatment from day 12. (D, F) The fold changes of immature megakaryocytic cells over each untreated sample (D) on day 9 and (F) on day 16 (n = 4 biologically independent experiments for Ts21-WT and n = 3 for Ts21-WT-Δex2). Data are presented as the mean ± SD. *$p < 0.05$ vs. Ts21-WT under same treatment by two-tailed unpaired Student's *t*-test.

S8 Fig. Over expression of GATA1s also has little effect on immature megakaryocytic cells of TAM-iPS-*GATA1*-WT derived cells.

(A) Representative flow cytometry of staining for CD34 and CD45 among myeloid cells on day 12. Upper panels indicate the Dox-untreated sample and lower panels indicate the Dox-treated sample from day 9. (B) The fold change of immature myeloid cells over untreated sample on day 12 and day 16. (C, E) Representative flow cytometry of staining for CD34 and CD41 (C) on day 9 with or without Dox treatment from day 6 and € on day 16 with or without Dox treatment from day 9. (D, F) The fold

679 changes of immature megakaryocytic cells over each untreated sample (D) on day 9 and (F) on day
680 16 (n = 3 biologically independent experiments). Data are presented as the mean ± SD. ***$p < 0.001$
681 vs. Ts21-WT under same treatment by two-tailed unpaired Student's *t*-test.
682
683 **S9 Fig. Conflicting effects of quantitative increase of GATA1s on commitment and persistence**
684 **is also observed in TAM-iPS-GATA1s derived cells.**
685 (A) Representative flow cytometry of staining for CD34 and CD41 on day 9. Upper panels indicate
686 the Dox-untreated sample and lower panels indicate the Dox-treated sample from day 6 for each clone.
687 (B) Fold changes of immature megakaryocytic cells over each untreated sample on day 9. (C)
688 Representative flow cytometry of staining for CD41 and CD42b on day 16 with or without Dox
689 treatment from day 9. (D) Fold changes of megakaryocytic cells over each untreated sample on day
690 16. (E) Representative flow cytometry of staining for CD34 and CD41 on day 16 with or without Dox
691 treatment from day 9. (F) Fold changes of immature megakaryocytic cells over each untreated sample
692 on day 16 (n = 3 biologically independent experiments). Data are presented as the mean ± SD. *$p <$
693 0.05, **$p < 0.01$ by two-tailed unpaired Student's *t*-test.
694
695 **S10 Fig. Erythroid differentiation defect of *GATA1s* is remarkably recovered by GATA1fl**
696 **overexpression in the early stage.**

(A) Representative flow cytometry of staining for CD34 and CD41 on day 9. Upper panels indicate the Dox-untreated sample and lower panels indicate the Dox-treated sample from day 6. (B) The fold changes of immature megakaryocytic cells over each untreated sample on day 9. (C) Representative flow cytometry of staining for CD71 and CD235a on day 16 with or without Dox treatment from day 6. (D) Average number of $CD235a^+$ erythrocytic cells on day 16 (n = 5 biologically independent experiments for Ts21-s and n = 3 for Ts21-s-fl). (E) May-Giemsa staining of Ts21-s-fl on day 16 with or without Dox treatment from day 6. Scale bars: 50 μm. Data are presented as the mean ± SD. $^{**}p < 0.01$, $^{***}p < 0.001$ vs. Ts21-s under same treatment by two-tailed unpaired Student's *t*-test.

S11 Fig. Erythroid differentiation defect is also remarkably recovered in TAM-iPS-*GATA1s* derived cells by GATA1fl overexpression.

(A) Representative flow cytometry of staining for CD34 and CD41 on day 9. Upper panels indicate the Dox-untreated sample and lower panels indicate the Dox-treated sample from day 6. (B) The fold changes of immature megakaryocytic cells over each untreated sample on day 9. (C) Representative flow cytometry of staining for CD71 and CD235a on day 16 with or without Dox treatment from day 6. (D) Average number of $CD235a^+$ erythrocytic cells on day 16 (n = 3 biologically independent experiments). (E) May-Giemsa staining of TAM-s-fl on day 16 with or without Dox treatment from day 6. Scale bars: 50 μm. Data are presented as the mean ± SD. $^{**}p < 0.01$, $^{***}p < 0.001$ vs. TAM-s

716 under same treatment by two-tailed unpaired Student's *t*-test.

717

718 **S12 Fig. The original uncropped and unadjusted gel and blot images.**

719 (A) The original image of electrophoretic gel of **S2B Fig**. lane 1, Marker; lane 2, water; lane 3, Ts21-

720 WT; lane 4, Ts21-WT-Δex2; lane 5, Ts21-s; lane 6, Ts21-s-Δex2; lane 7 – 8, not shown. (B, C) Original

721 uncut gel images of western blot analysis. (B) Ts21-ES clones on **Fig 2C**; lane 1 – 7, not shown; lane

722 8, Marker; lane 9, Ts21-WT-Δex2 Dox (-); lane 10, Ts21-WT-Δex2 Dox (+); lane 11, Ts21-s-Δex2

723 Dox (-); lane 12, Ts21-s-Δex2 Dox (+); lane 13, Ts21-s-fl Dox (-); lane 14, Ts21-s-fl Dox (+); lane 15,

724 K562. (B) TAM-iPS clones on **S4G Fig**; lane 1, Marker; lane 2, TAM-WT-Δex2 Dox (-); lane 3, TAM-

725 WT-Δex2 Dox (+); lane 4, TAM-s-Δex2 Dox (-); lane 5, TAM-s-Δex2 Dox (+); lane 6, TAM-s-fl Dox

726 (-); lane 7, TAM-s-fl Dox (+); lane 8, K562.

727

Fig 1

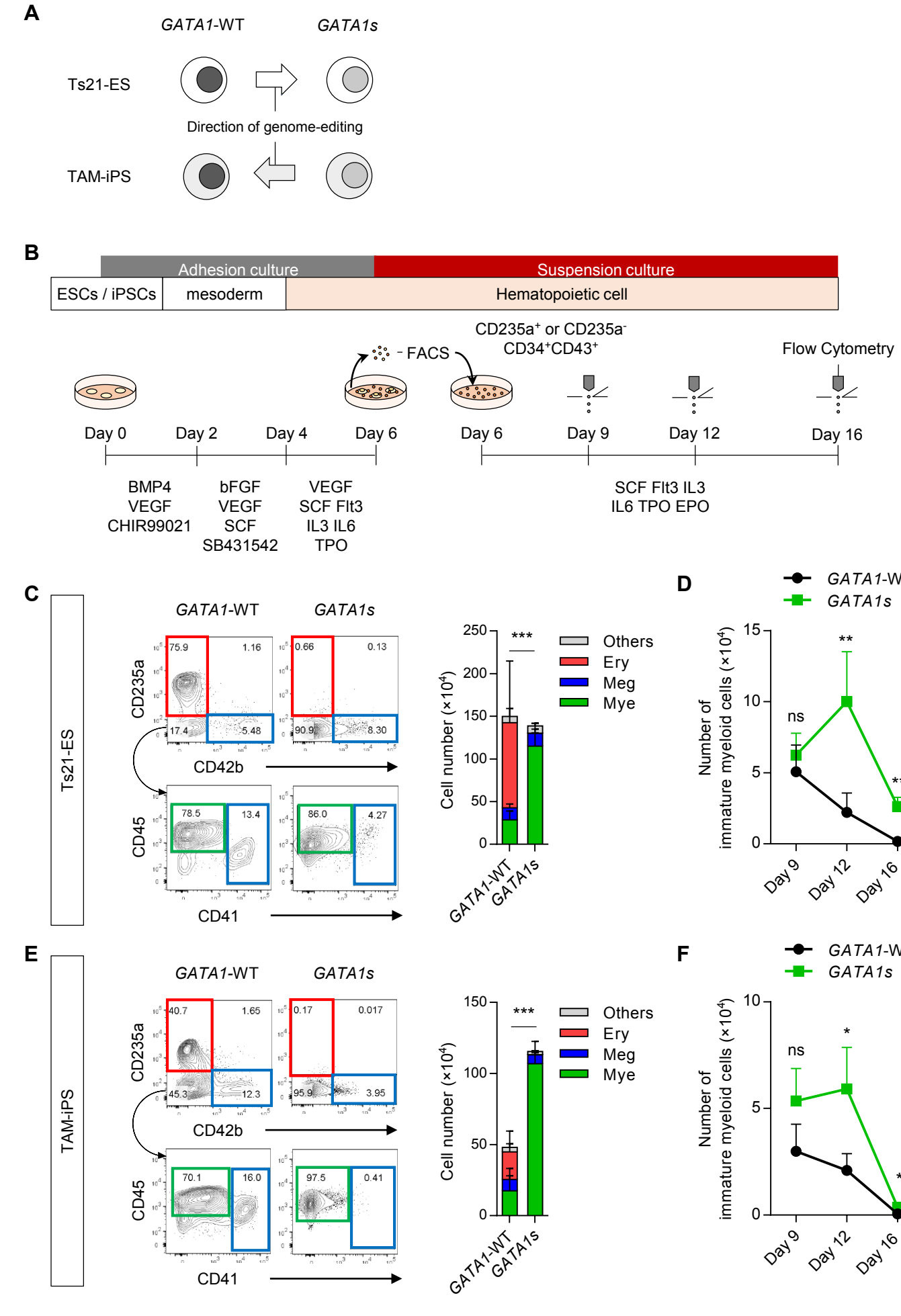
A
GATA1-WT
GATA1s
Ts21-ES
Direction of genome-editing
TAM-iPS
B
Adhesion culture
Suspension culture
ESCs / iPSCs
mesoderm
Hematopoietic cell
FACS
CD235a+ or CD235a-
CD34+CD43+
Flow Cytometry
Day 0
Day 2
Day 4
Day 6
Day 6
Day 9
Day 12
Day 16
BMP4
VEGF
CHIR99021
bFGF
VEGF
SCF
SB431542
VEGF
SCF Flt3
IL3 IL6
TPO
SCF Flt3 IL3
IL6 TPO EPO
C
Ts21-ES
GATA1-WT
GATA1s
CD235a
CD42b
CD45
CD41
75.9
1.16
17.4
5.48
0.66
0.13
90.9
8.30
78.5
13.4
86.0
4.27
Cell number (×10^4)
***
Others
Ery
Meg
Mye
GATA1-WT
GATA1s
D
GATA1-WT
GATA1s
Number of immature myeloid cells (×10^4)
ns
**
****
Day 9
Day 12
Day 16
E
TAM-iPS
GATA1-WT
GATA1s
CD235a
CD42b
CD45
CD41
40.7
1.65
45.3
12.3
0.17
0.017
95.9
3.95
70.1
16.0
97.5
0.41
Cell number (×10^4)
***
Others
Ery
Meg
Mye
GATA1-WT
GATA1s
F
GATA1-WT
GATA1s
Number of immature myeloid cells (×10^4)
ns
*
**
Day 9
Day 12
Day 16

Fig 2

A

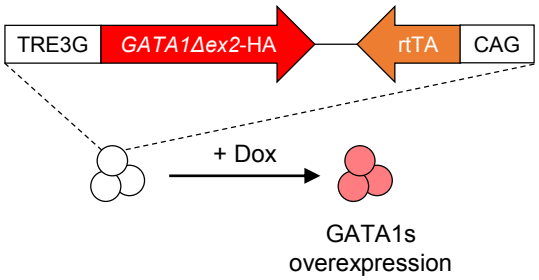
TRE3G
GATA1Δex2-HA
rtTA
CAG
+ Dox
GATA1s
overexpression

B

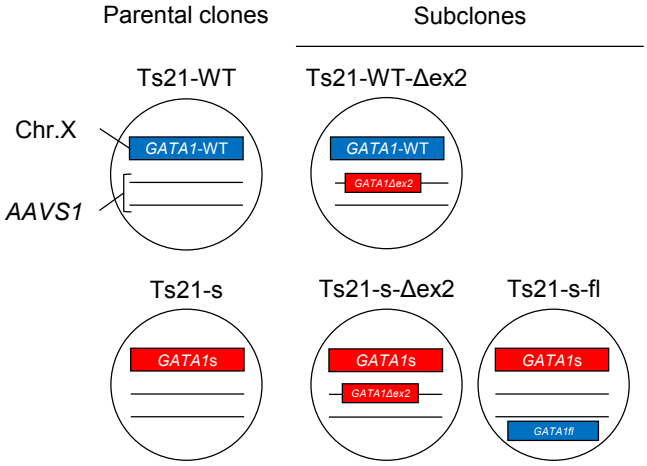
Parental clones
Subclones
Ts21-WT
Ts21-WT-Δex2
Chr.X
AAVS1
GATA1-WT
GATA1Δex2
Ts21-s
Ts21-s-Δex2
Ts21-s-fl
GATA1s
GATA1fl

C

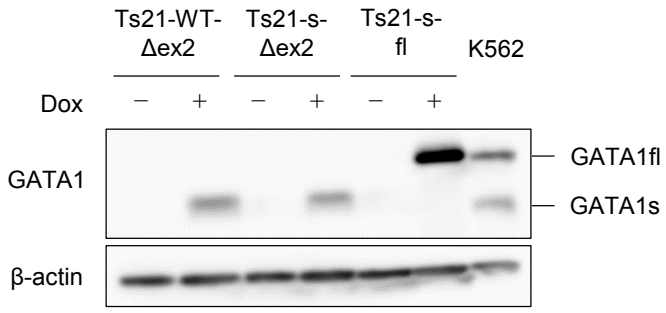
Ts21-WT-Δex2
Ts21-s-Δex2
Ts21-s-fl
K562
Dox
− + − + − +
GATA1
β-actin
GATA1fl
GATA1s

Fig 3

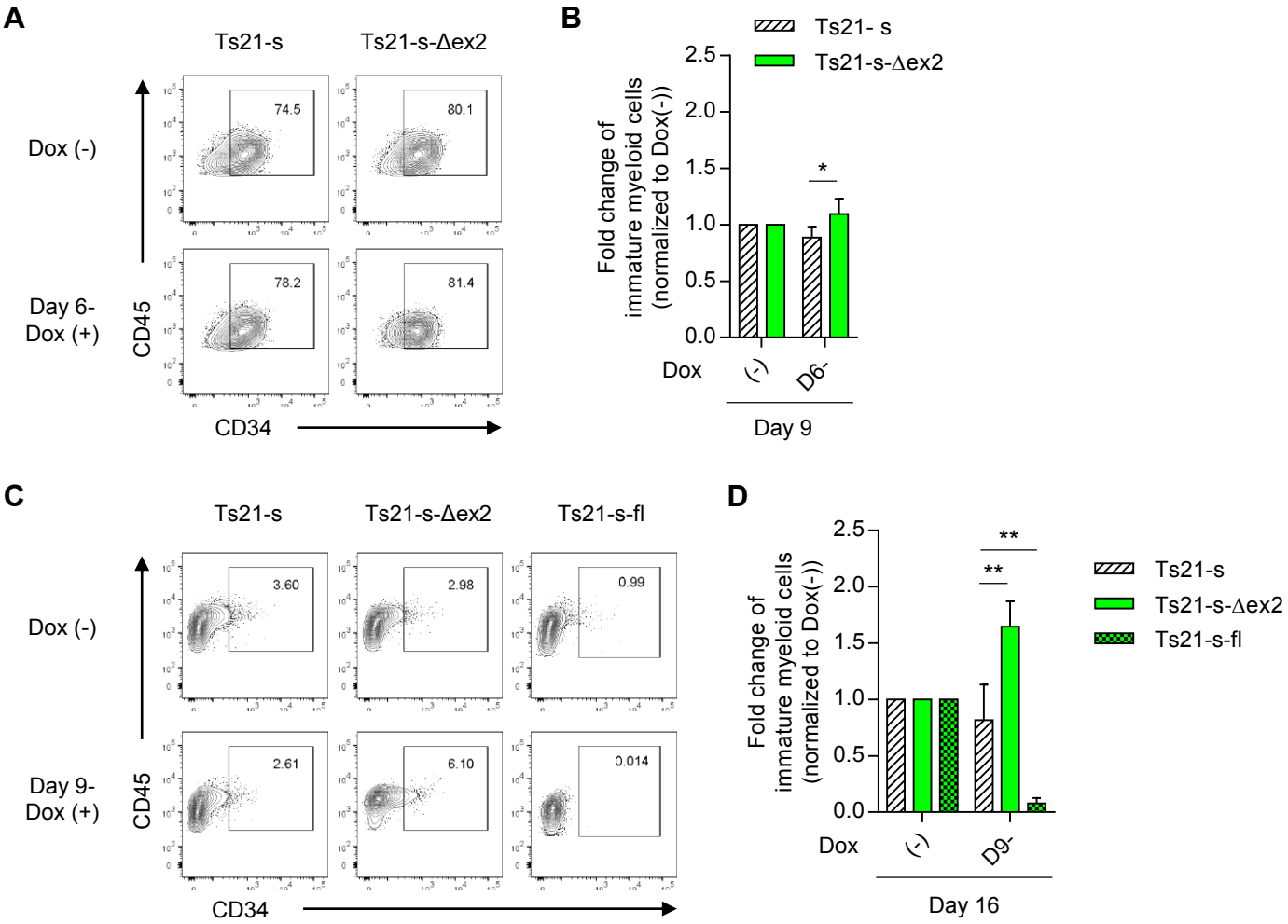
A
Ts21-s
Ts21-s-Δex2
Dox (-)
Day 6-
Dox (+)
74.5
80.1
78.2
81.4
CD45
CD34
B
Ts21- s
Ts21-s-Δex2
Fold change of
immature myeloid cells
(normalized to Dox(-))
2.5
2.0
1.5
1.0
0.5
0.0
*
Dox
(-)
D6
Day 9
C
Ts21-s
Ts21-s-Δex2
Ts21-s-fl
Dox (-)
Day 9-
Dox (+)
3.60
2.98
0.99
2.61
6.10
0.014
CD45
CD34
D
Fold change of
immature myeloid cells
(normalized to Dox(-))
2.5
2.0
1.5
1.0
0.5
0.0
**
**
Dox
(-)
D9
Day 16
Ts21-s
Ts21-s-Δex2
Ts21-s-fl

Fig 4

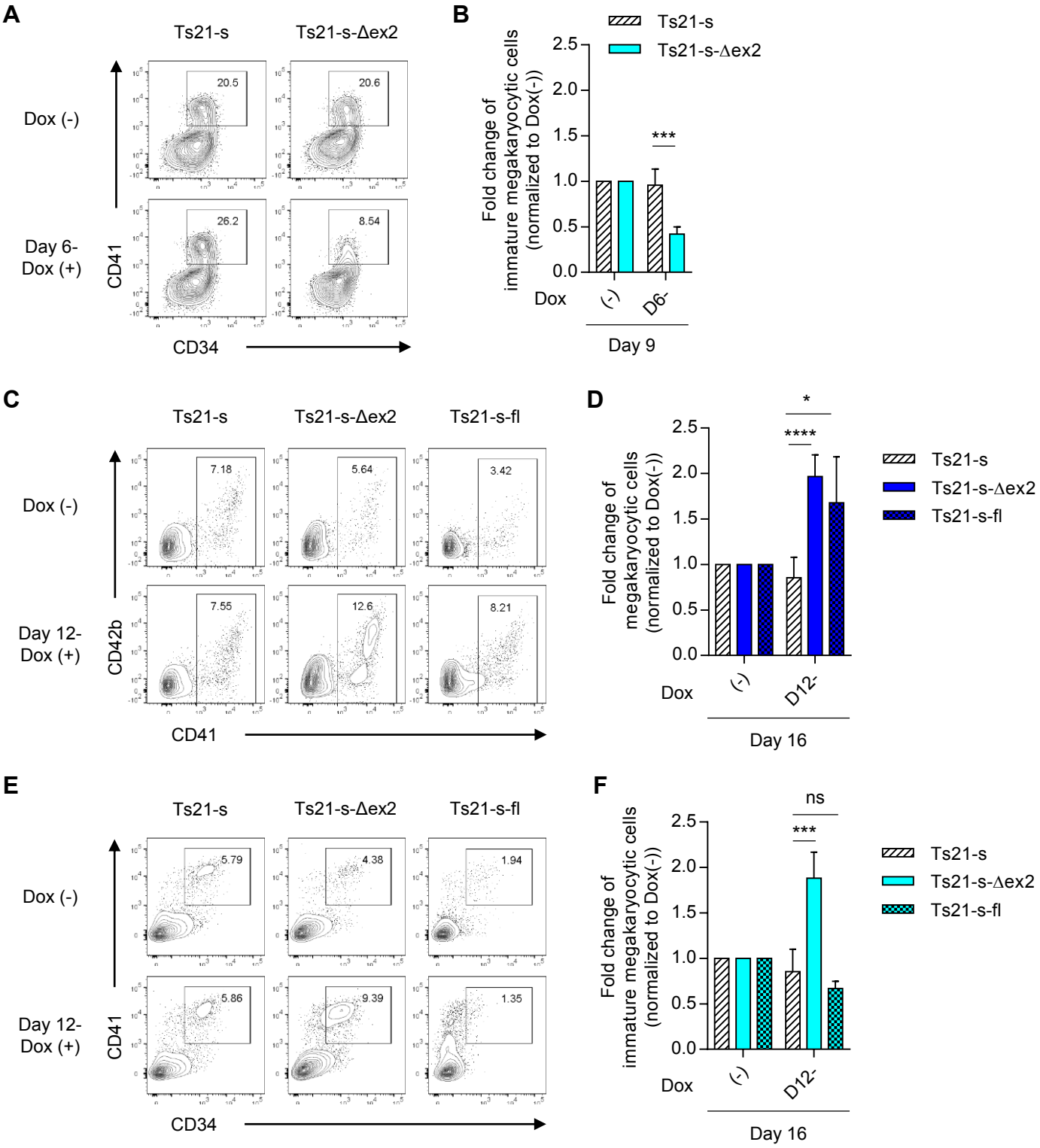
A
Ts21-s
Ts21-s-Δex2
Dox (-)
Day 6-
Dox (+)
CD41
CD34
20.5
20.6
26.2
8.54
B
Ts21-s
Ts21-s-Δex2
Fold change of
immature megakaryocytic cells
(normalized to Dox(-))
***
Dox
(-)
D6-
Day 9
C
Ts21-s
Ts21-s-Δex2
Ts21-s-fl
Dox (-)
Day 12-
Dox (+)
CD42b
CD41
7.18
5.64
3.42
7.55
12.6
8.21
D
*
****
Fold change of
megakaryocytic cells
(normalized to Dox(-))
Dox
(-)
D12-
Day 16
Ts21-s
Ts21-s-Δex2
Ts21-s-fl
E
Ts21-s
Ts21-s-Δex2
Ts21-s-fl
Dox (-)
Day 12-
Dox (+)
CD41
CD34
5.79
4.38
1.94
5.86
9.39
1.35
F
ns
***
Fold change of
immature megakaryocytic cells
(normalized to Dox(-))
Dox
(-)
D12-
Day 16
Ts21-s
Ts21-s-Δex2
Ts21-s-fl

Fig 5

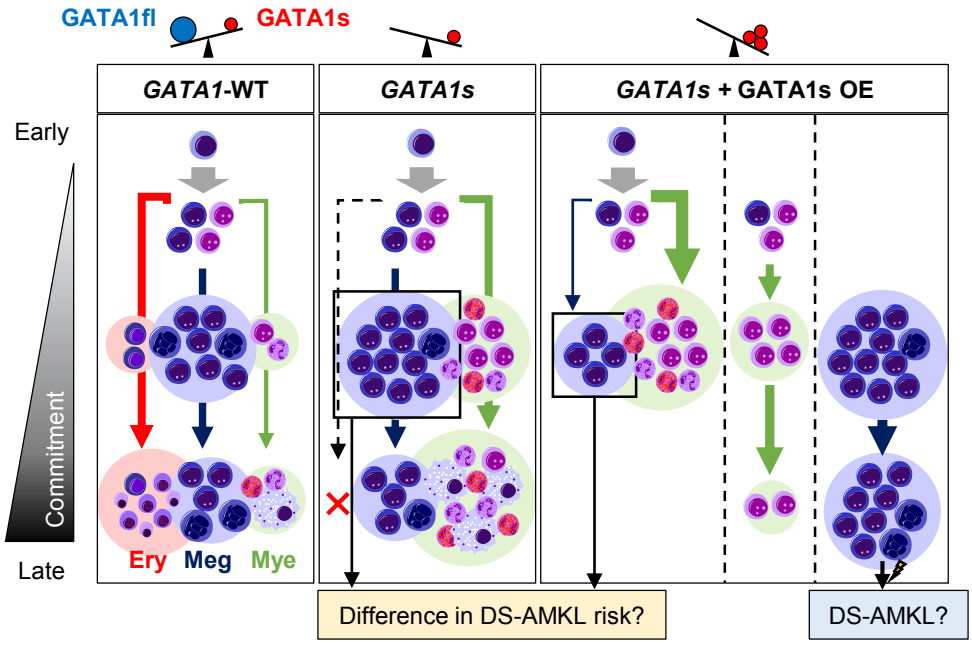
GATA1fl
GATA1s
GATA1-WT
GATA1s
GATA1s + GATA1s OE
Early
Commitment
Late
Ery
Meg
Mye
Difference in DS-AMKL risk?
DS-AMKL?

S1 Fig

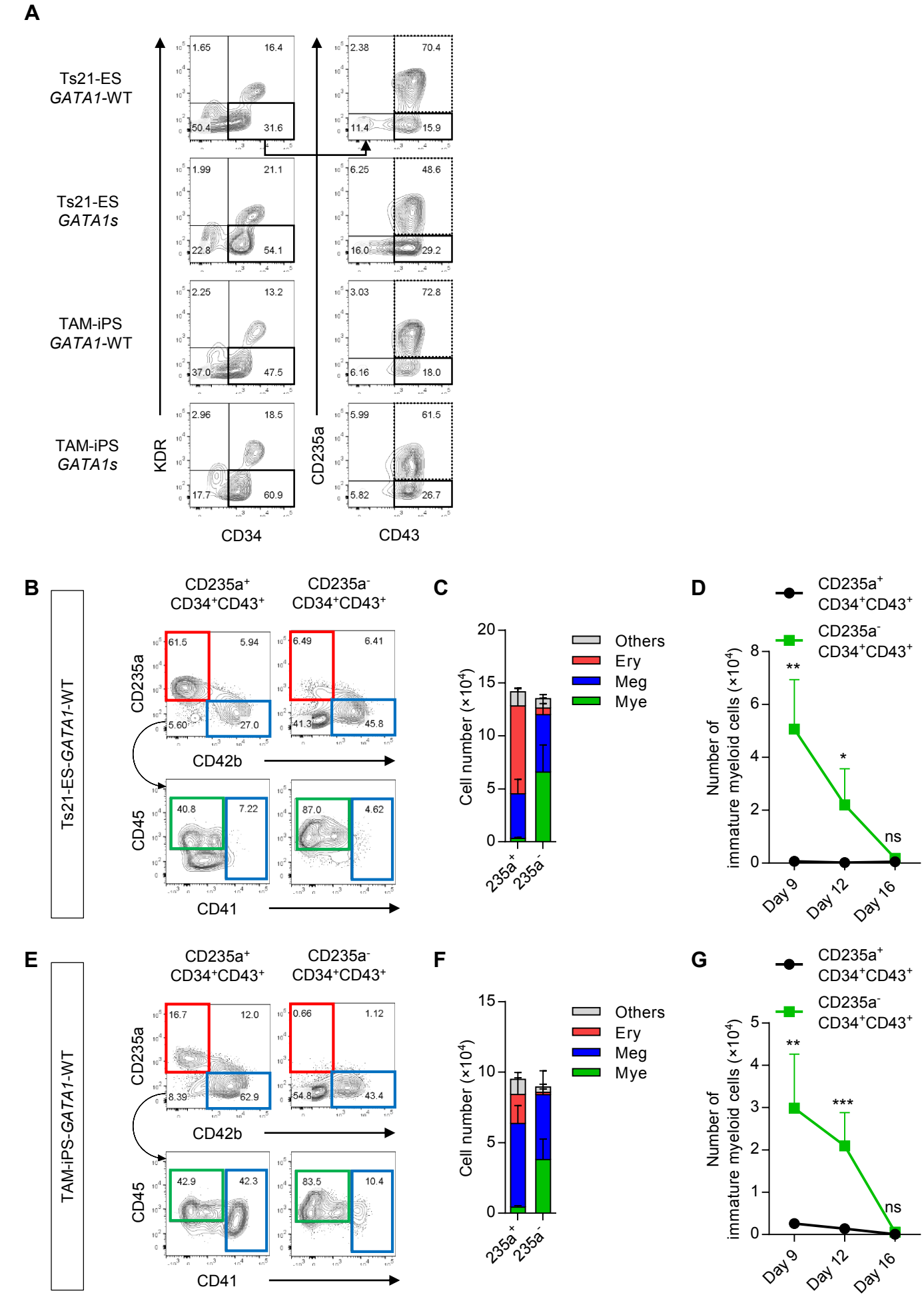
A
Ts21-ES
GATA1-WT
Ts21-ES
GATA1s
TAM-iPS
GATA1-WT
TAM-iPS
GATA1s
KDR
CD34
CD235a
CD43
1.65
16.4
50.4
31.6
2.38
70.4
11.4
15.9
1.99
21.1
22.8
54.1
6.25
48.6
16.0
29.2
2.25
13.2
37.0
47.5
3.03
72.8
6.16
18.0
2.96
18.5
17.7
60.9
5.99
61.5
5.82
26.7
B
Ts21-ES-GATA1-WT
CD235a+ CD34+CD43+
CD235a- CD34+CD43+
CD235a
CD42b
CD45
CD41
61.5
5.94
5.60
27.0
6.49
6.41
41.3
45.8
40.8
7.22
87.0
4.62
C
Cell number (×10^4)
Others
Ery
Meg
Mye
235a+
235a-
D
CD235a+ CD34+CD43+
CD235a- CD34+CD43+
Number of immature myeloid cells (×10^4)
Day 9
Day 12
Day 16
**
*
ns
E
TAM-iPS-GATA1-WT
CD235a+ CD34+CD43+
CD235a- CD34+CD43+
CD235a
CD42b
CD45
CD41
16.7
12.0
8.39
62.9
0.66
1.12
54.8
43.4
42.9
42.3
83.5
10.4
F
Cell number (×10^4)
Others
Ery
Meg
Mye
235a+
235a-
G
CD235a+ CD34+CD43+
CD235a- CD34+CD43+
Number of immature myeloid cells (×10^4)
Day 9
Day 12
Day 16
**
***
ns

S2 Fig

A

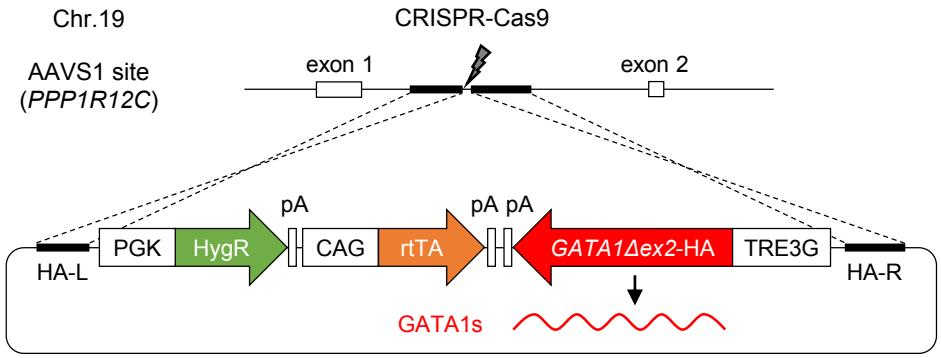

B

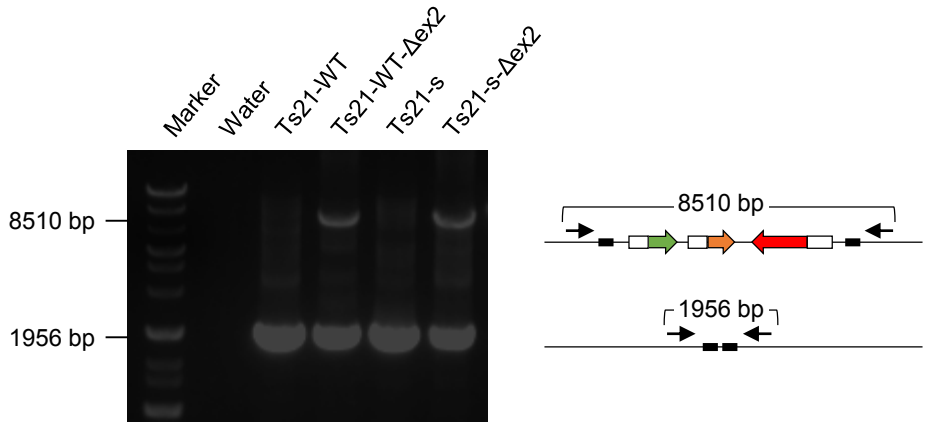

C

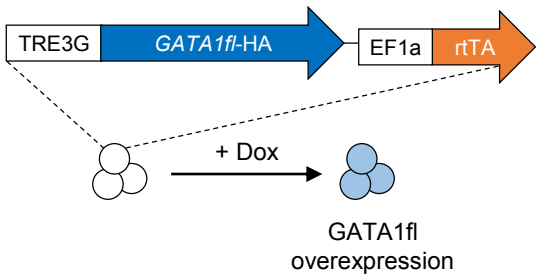

PiggyBac vector

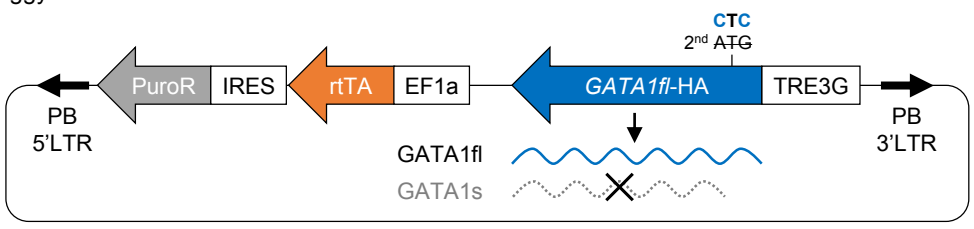

S3 Fig

A Ts21-ES-*GATA1*-WT

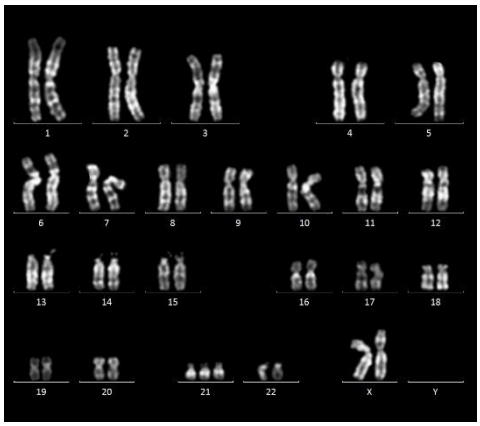

B Ts21-ES-*GATA1s*

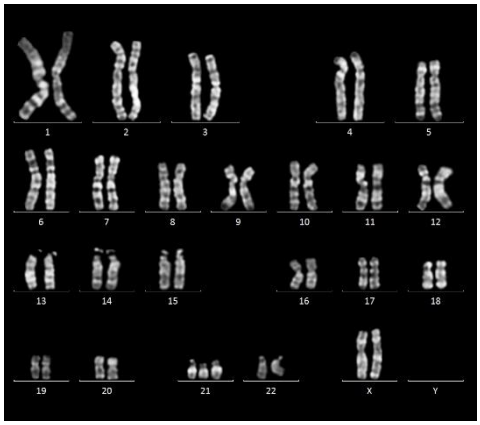

C Ts21-WT-Δex2

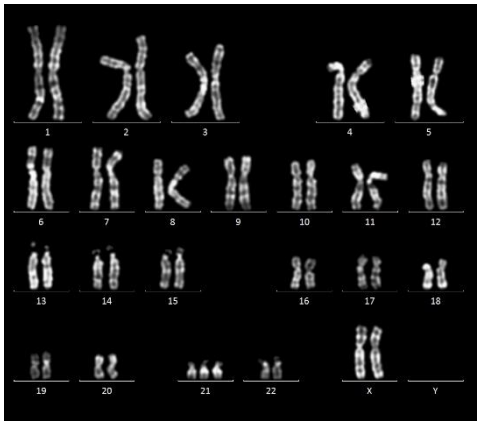

D Ts21-s-Δex2

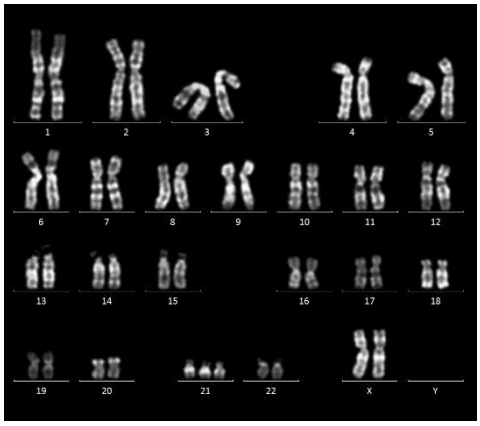

E Ts21-s-fl

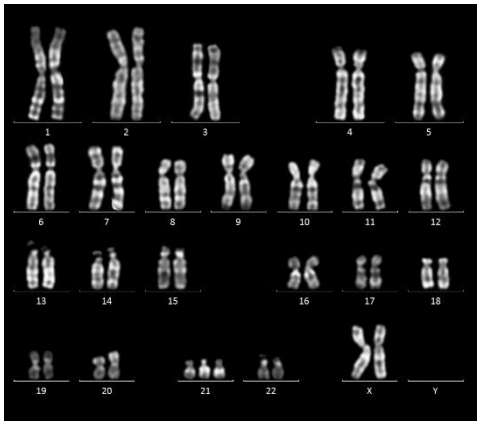

S4 Fig

A

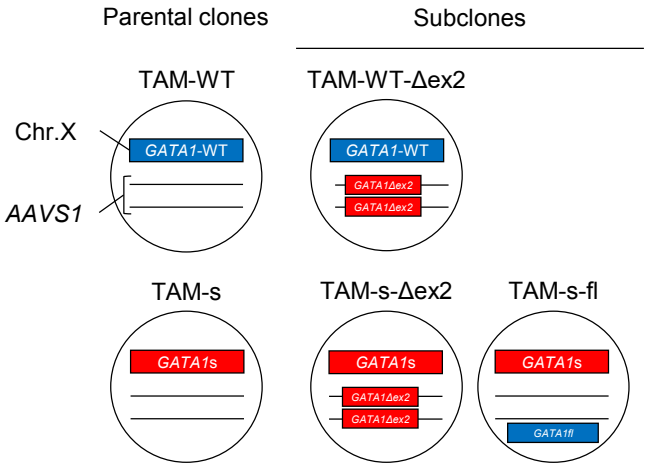

B TAM-iPS-*GATA1*-WT

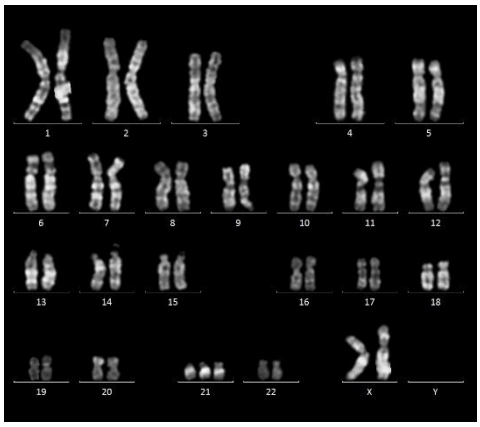

C TAM-iPS-*GATA1s*

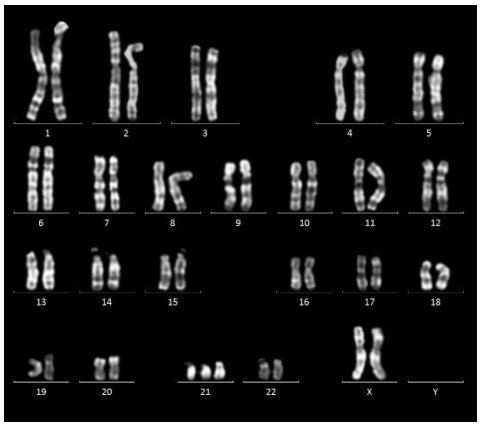

D TAM-WT-Δex2

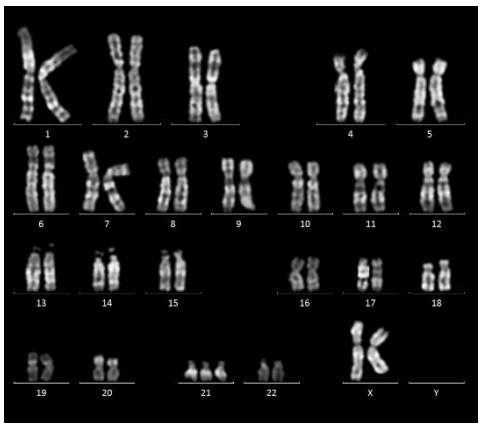

E TAM-s-Δex2

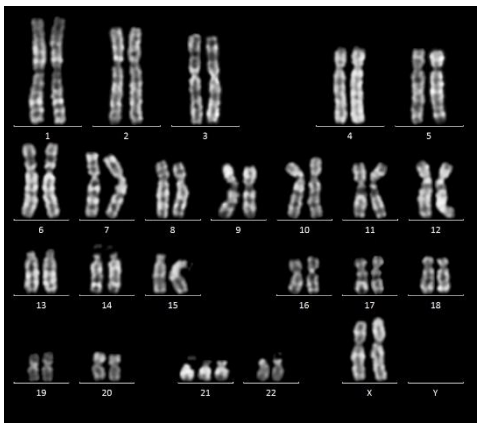

F TAM-s-fl

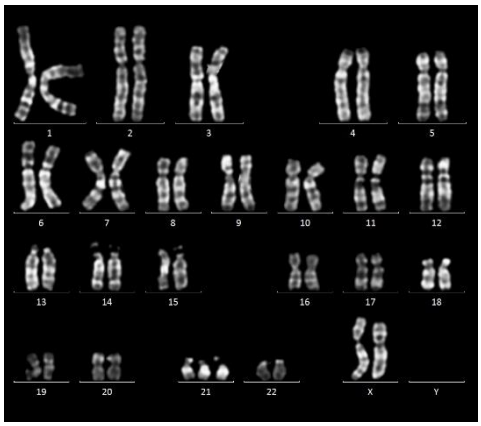

G

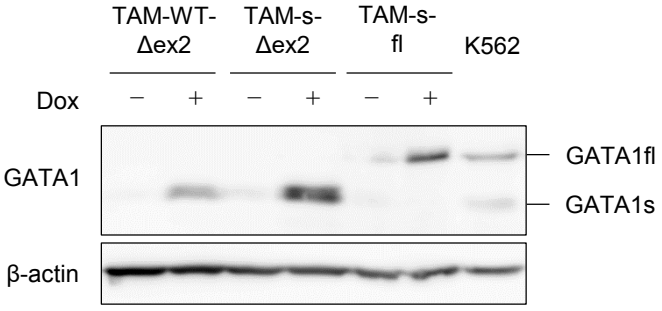

S5 Fig

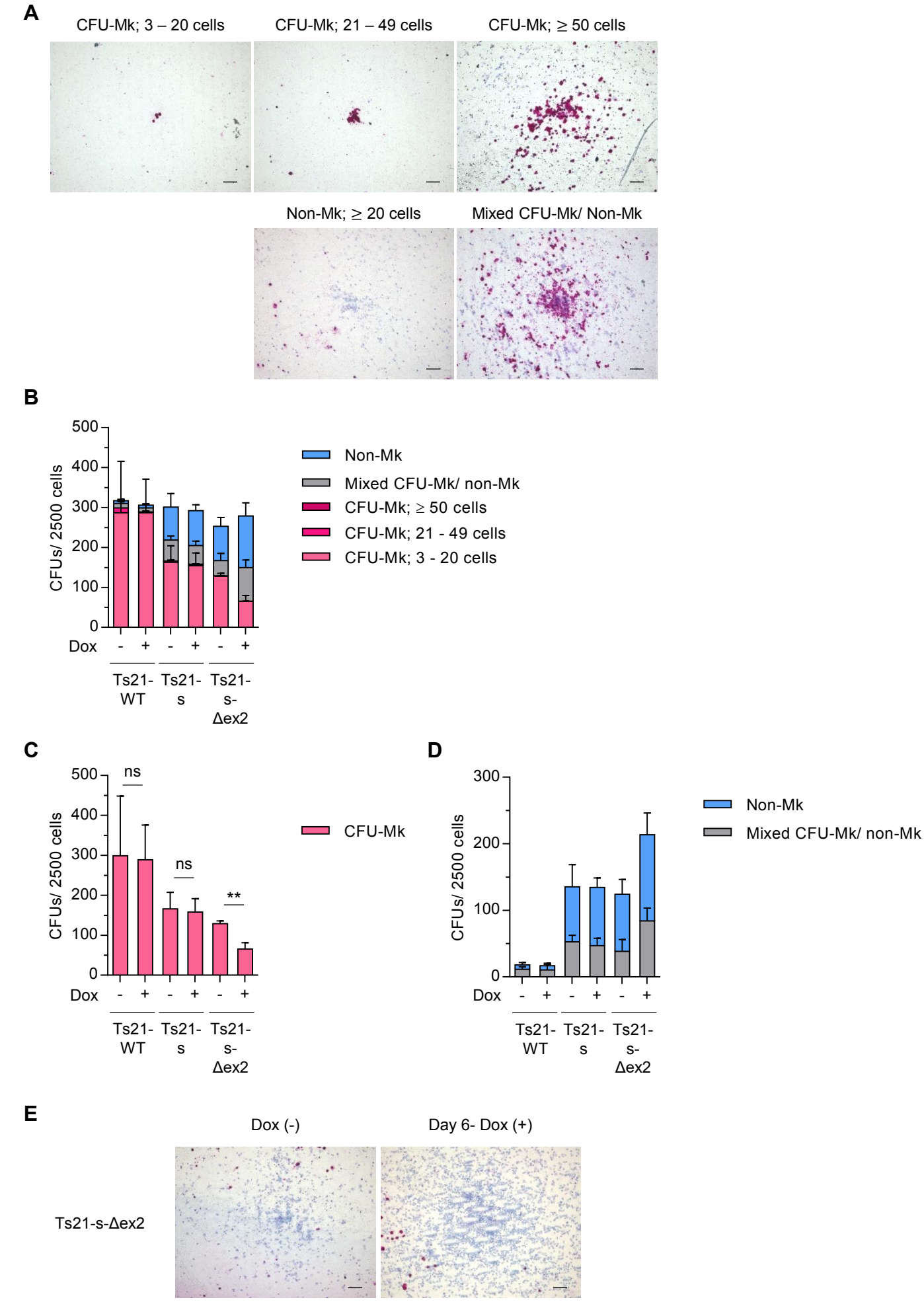
A
CFU-Mk; 3 – 20 cells
CFU-Mk; 21 – 49 cells
CFU-Mk; ≥ 50 cells
Non-Mk; ≥ 20 cells
Mixed CFU-Mk/ Non-Mk
B
CFUs/ 2500 cells
500
400
300
200
100
0
Dox
- + - + - +
Ts21-WT
Ts21-s
Ts21-s-Δex2
Non-Mk
Mixed CFU-Mk/ non-Mk
CFU-Mk; ≥ 50 cells
CFU-Mk; 21 - 49 cells
CFU-Mk; 3 - 20 cells
C
ns
ns
**
CFU-Mk
D
Non-Mk
Mixed CFU-Mk/ non-Mk
E
Dox (-)
Day 6- Dox (+)
Ts21-s-Δex2

S6 Fig

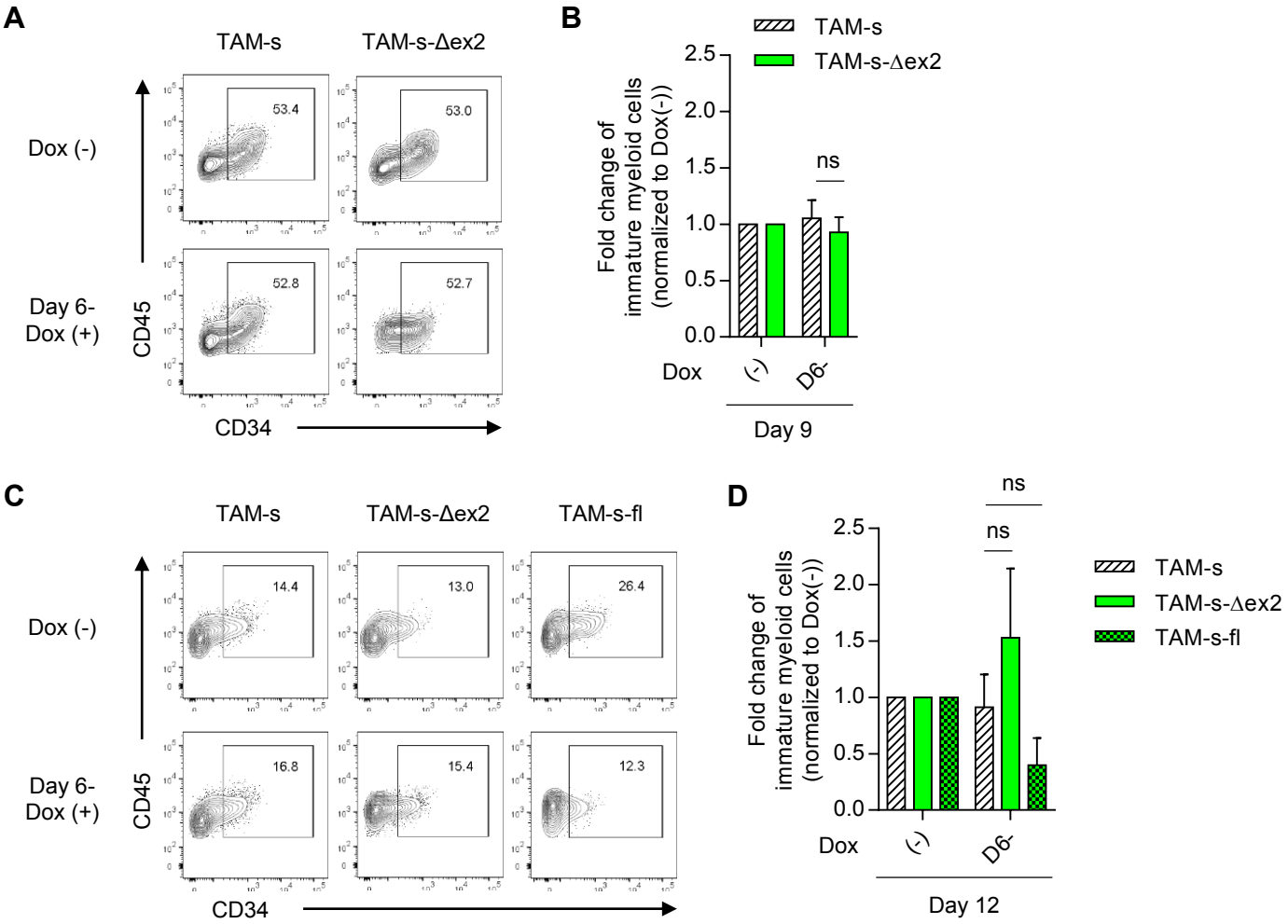
A
TAM-s
TAM-s-Δex2
Dox (-)
Day 6-
Dox (+)
CD45
CD34
53.4
53.0
52.8
52.7
B
TAM-s
TAM-s-Δex2
Fold change of
immature myeloid cells
(normalized to Dox(-))
2.5
2.0
1.5
1.0
0.5
0.0
ns
Dox
(-)
D6
Day 9
C
TAM-s
TAM-s-Δex2
TAM-s-fl
Dox (-)
Day 6-
Dox (+)
CD45
CD34
14.4
13.0
26.4
16.8
15.4
12.3
D
ns
ns
Fold change of
immature myeloid cells
(normalized to Dox(-))
2.5
2.0
1.5
1.0
0.5
0.0
Dox
(-)
D6
Day 12
TAM-s
TAM-s-Δex2
TAM-s-fl

S7 Fig

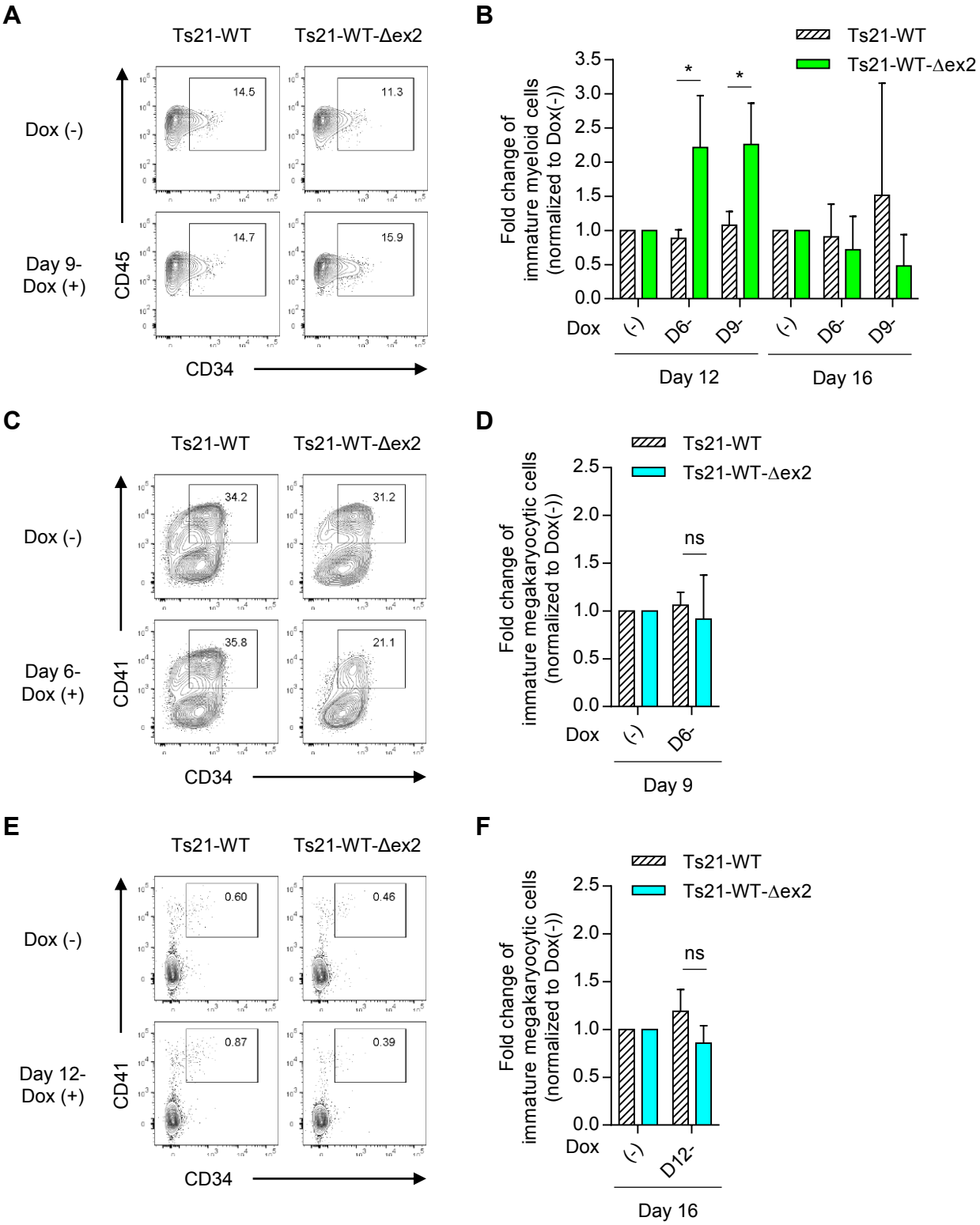
A
Ts21-WT
Ts21-WT-Δex2
Dox (-)
Day 9-
Dox (+)
CD45
CD34
14.5
11.3
14.7
15.9
B
Ts21-WT
Ts21-WT-Δex2
Fold change of
immature myeloid cells
(normalized to Dox(-))
3.5
3.0
2.5
2.0
1.5
1.0
0.5
0.0
*
*
Dox
(-)
D6-
D9-
(-)
D6-
D9-
Day 12
Day 16
C
Ts21-WT
Ts21-WT-Δex2
Dox (-)
Day 6-
Dox (+)
CD41
CD34
34.2
31.2
35.8
21.1
D
Ts21-WT
Ts21-WT-Δex2
Fold change of
immature megakaryocytic cells
(normalized to Dox(-))
2.5
2.0
1.5
1.0
0.5
0.0
ns
Dox
(-)
D6-
Day 9
E
Ts21-WT
Ts21-WT-Δex2
Dox (-)
Day 12-
Dox (+)
CD41
CD34
0.60
0.46
0.87
0.39
F
Ts21-WT
Ts21-WT-Δex2
Fold change of
immature megakaryocytic cells
(normalized to Dox(-))
2.5
2.0
1.5
1.0
0.5
0.0
ns
Dox
(-)
D12-
Day 16

S8 Fig

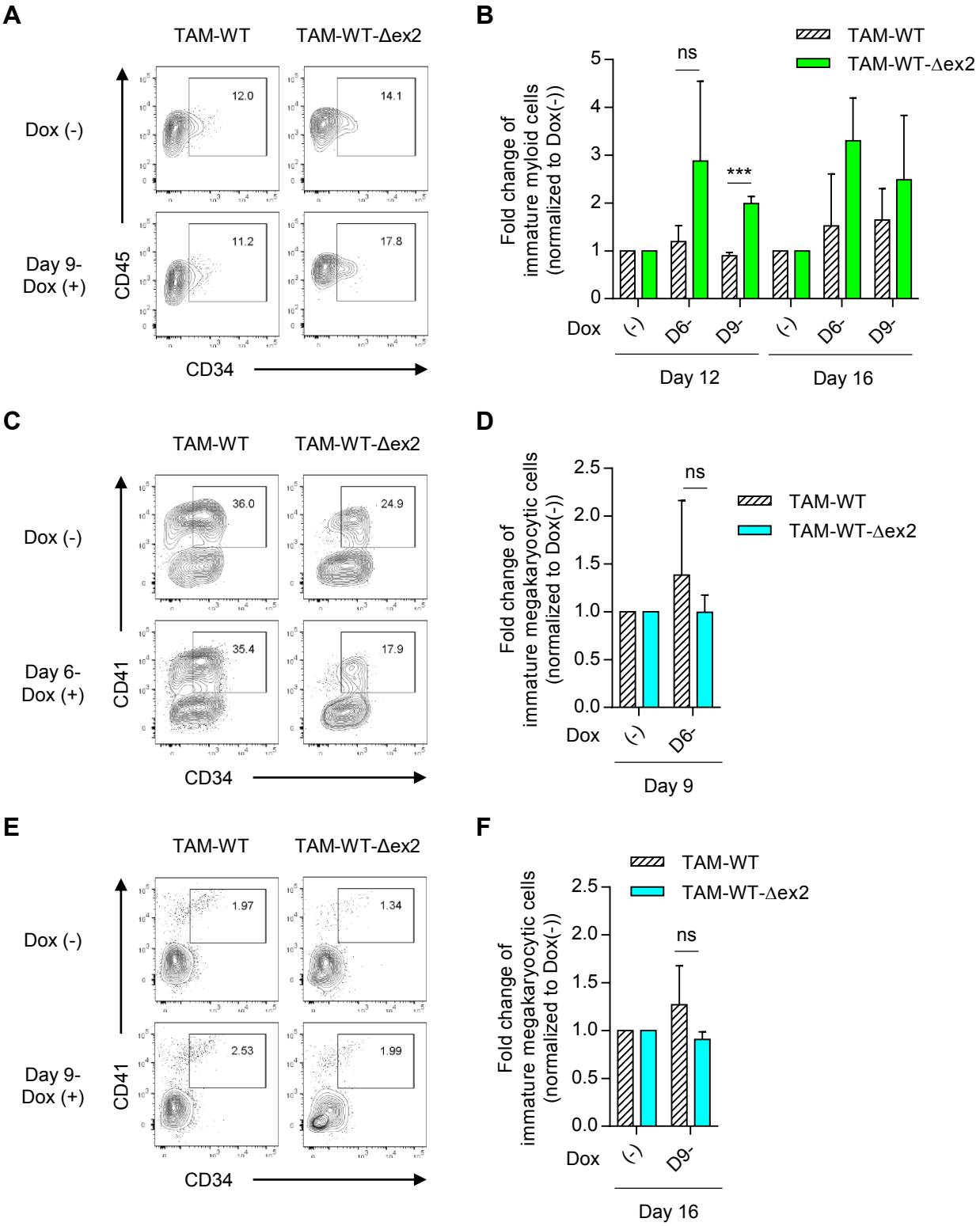
A
TAM-WT
TAM-WT-Δex2
Dox (-)
Day 9-
Dox (+)
CD45
CD34
12.0
14.1
11.2
17.8
B
TAM-WT
TAM-WT-Δex2
Fold change of
immature myloid cells
(normalized to Dox(-))
ns
***
Dox
(-)
D6-
D9-
Day 12
Day 16
C
TAM-WT
TAM-WT-Δex2
Dox (-)
Day 6-
Dox (+)
CD41
CD34
36.0
24.9
35.4
17.9
D
Fold change of
immature megakaryocytic cells
(normalized to Dox(-))
ns
TAM-WT
TAM-WT-Δex2
Dox
(-)
D6-
Day 9
E
TAM-WT
TAM-WT-Δex2
Dox (-)
Day 9-
Dox (+)
CD41
CD34
1.97
1.34
2.53
1.99
F
TAM-WT
TAM-WT-Δex2
Fold change of
immature megakaryocytic cells
(normalized to Dox(-))
ns
Dox
(-)
D9-
Day 16

S9 Fig

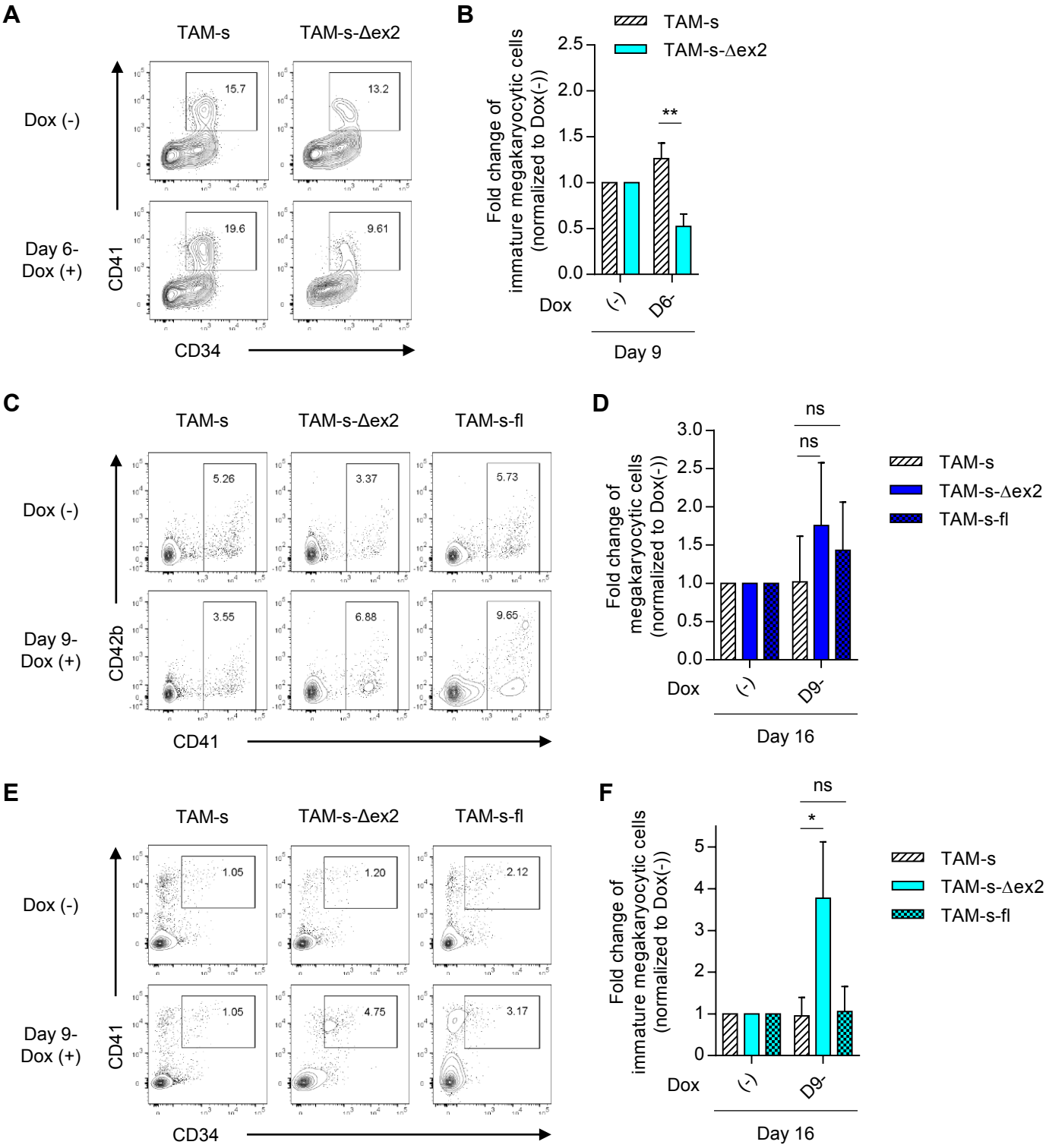
A
TAM-s
TAM-s-Δex2
Dox (-)
Day 6-
Dox (+)
CD41
CD34
15.7
13.2
19.6
9.61
B
TAM-s
TAM-s-Δex2
Fold change of
immature megakaryocytic cells
(normalized to Dox(-))
2.5
2.0
1.5
1.0
0.5
0.0
**
Dox
(-)
D6
Day 9
C
TAM-s
TAM-s-Δex2
TAM-s-fl
Dox (-)
Day 9-
Dox (+)
CD42b
CD41
5.26
3.37
5.73
3.55
6.88
9.65
D
ns
ns
Fold change of
megakaryocytic cells
(normalized to Dox(-))
3.0
2.5
2.0
1.5
1.0
0.5
0.0
Dox
(-)
D9
Day 16
TAM-s
TAM-s-Δex2
TAM-s-fl
E
TAM-s
TAM-s-Δex2
TAM-s-fl
Dox (-)
Day 9-
Dox (+)
CD41
CD34
1.05
1.20
2.12
1.05
4.75
3.17
F
ns
*
Fold change of
immature megakaryocytic cells
(normalized to Dox(-))
5
4
3
2
1
0
Dox
(-)
D9
Day 16
TAM-s
TAM-s-Δex2
TAM-s-fl

S10 Fig

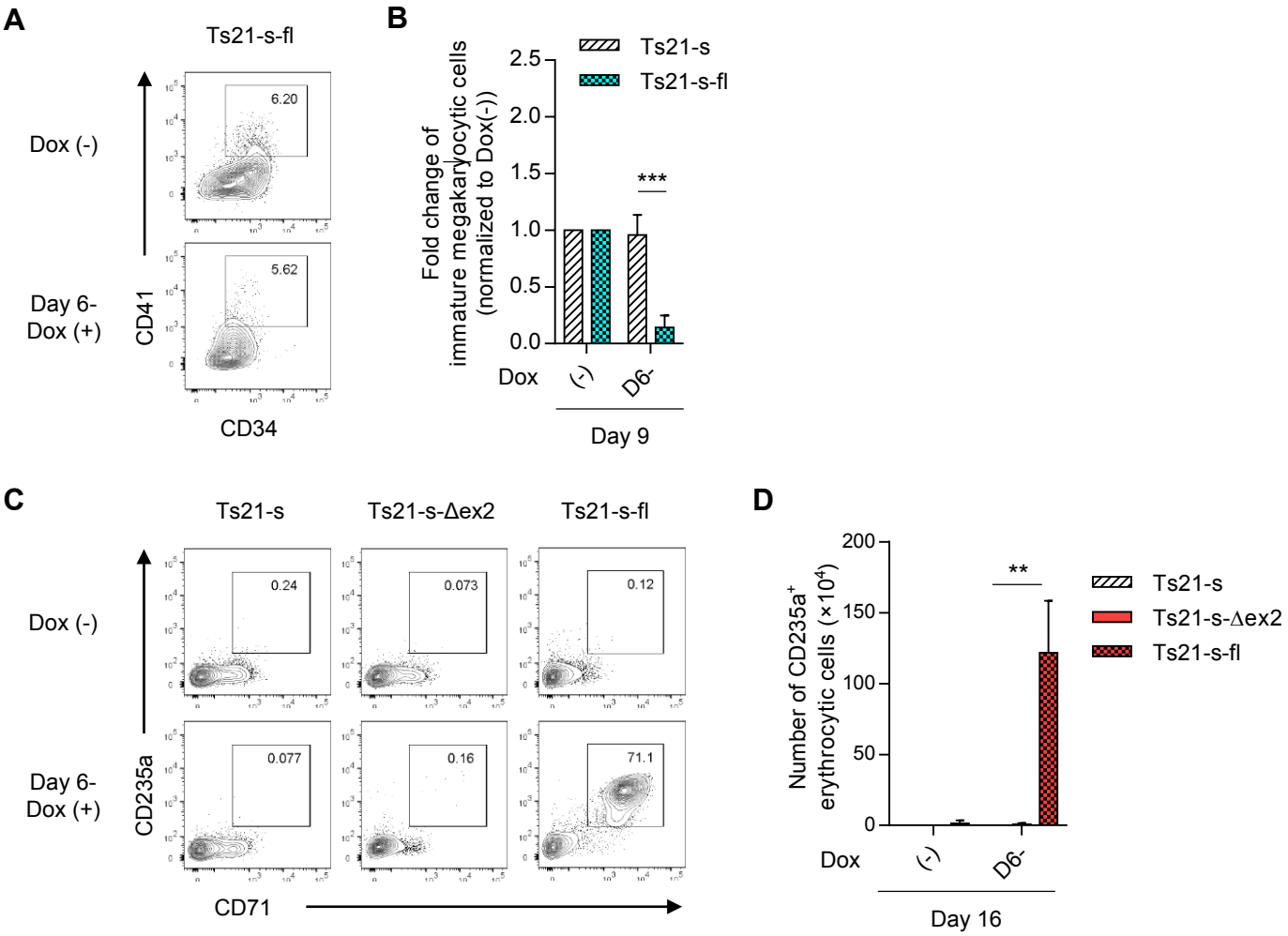
A
Ts21-s-fl
Dox (-)
Day 6-
Dox (+)
6.20
5.62
CD41
CD34
B
Ts21-s
Ts21-s-fl
Fold change of
immature megakaryocytic cells
(normalized to Dox(-))
2.5
2.0
1.5
1.0
0.5
0.0
***
Dox
(-)
D6
Day 9
C
Ts21-s
Ts21-s-Δex2
Ts21-s-fl
Dox (-)
Day 6-
Dox (+)
0.24
0.073
0.12
0.077
0.16
71.1
CD235a
CD71
D
Number of CD235a+
erythrocytic cells (×10⁴)
200
150
100
50
0
**
Ts21-s
Ts21-s-Δex2
Ts21-s-fl
Dox
(-)
D6
Day 16
E
Dox (-)
Day 6- Dox (+)
Ts21-s-fl

S11 Fig

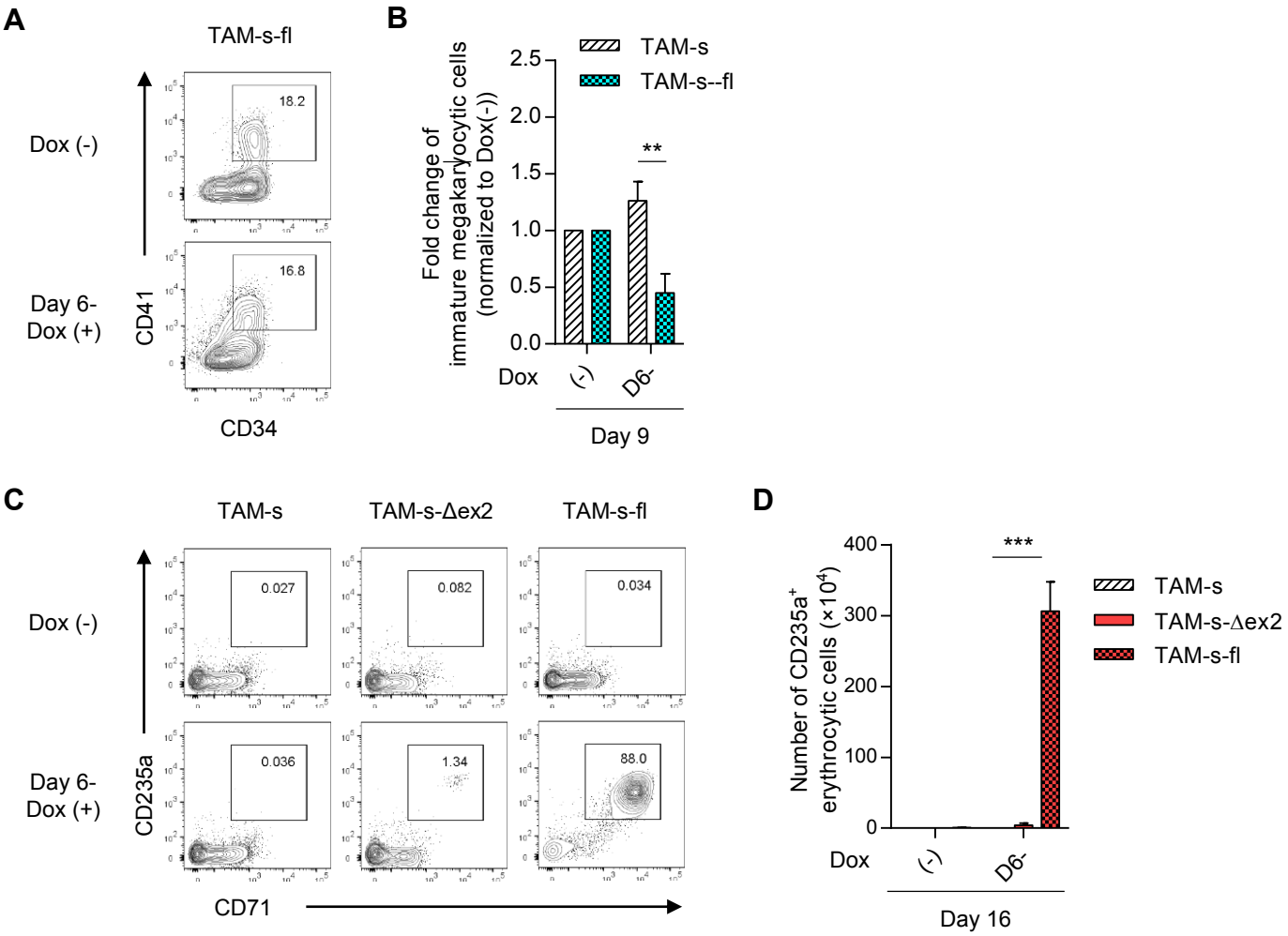
A
TAM-s-fl
Dox (-)
Day 6-
Dox (+)
18.2
16.8
CD41
CD34
B
TAM-s
TAM-s--fl
Fold change of
immature megakaryocytic cells
(normalized to Dox(-))
2.5
2.0
1.5
1.0
0.5
0.0
**
Dox
(-)
D6-
Day 9
C
TAM-s
TAM-s-Δex2
TAM-s-fl
Dox (-)
Day 6-
Dox (+)
0.027
0.082
0.034
0.036
1.34
88.0
CD235a
CD71
D
Number of CD235a+
erythrocytic cells (×10^4)
400
300
200
100
0
***
Dox
(-)
D6-
Day 16
TAM-s
TAM-s-Δex2
TAM-s-fl
E
Dox (-)
Day 6- Dox (+)
TAM-s-fl

S12 Fig

A

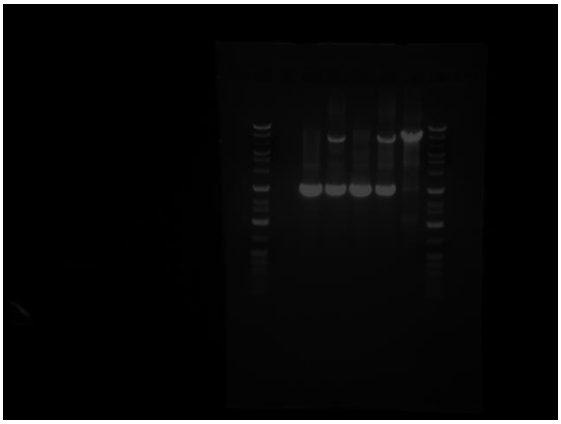

B

GATA1

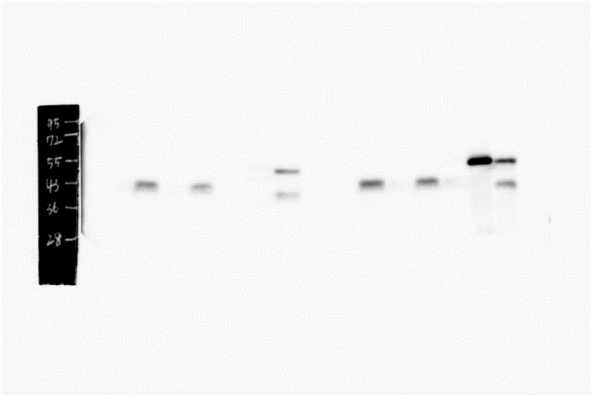

β-actin

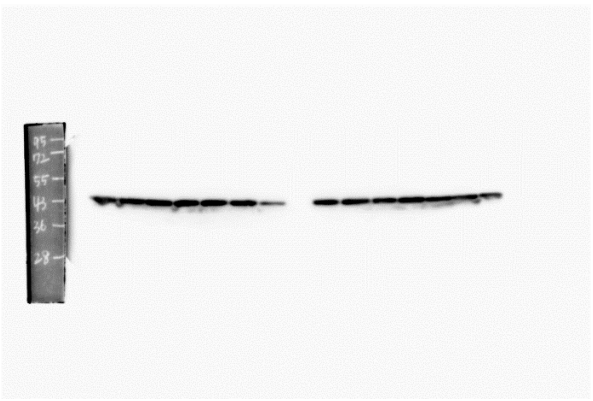

C